

## CXCL1, CCL20, STAT1 was Identified and Validated as a Key Biomarker Related to Immunity in Patients with Ulcerative Colitis

Wendi Xu, Dongju Long, Shapaer Tiannake, Yuhong Jiang, Tong Han, Xiaobo Wang, and Kuijie Liu\*

Department of General Surgery, The Second Xiangya Hospital, Central South University, No.139 Middle Renmin Road, Changsha, Hunan 410011, P.R. China

### \*Corresponding author:

Kuijie Liu,  
Department of General Surgery, The Second  
Xiangya Hospital, Central South University,  
No.139 Middle Renmin Road, Changsha, Hunan  
410011, P.R. China, E-mail: liukuijie@csu.edu.cn

Received: 17 Nov 2021  
Accepted: 16 Dec 2021  
Published: 21 Dec 2021  
J Short Name: COS

### Copyright:

©2021 Kuijie Liu. This is an open access article distributed under the terms of the Creative Commons Attribution License, which permits unrestricted use, distribution, and build upon your work non-commercially.

### Citation:

Kuijie Liu, CXCL1, CCL20, STAT1 was Identified and Validated as a Key Biomarker Related to Immunity in Patients with Ulcerative Colitis. Clin Surg. 2021; 6(13): 1-29

### Keywords:

Ulcerative colitis; Immune-related gene; WGCAN; Biomarker

### 1. Abstract

**1.1. Background:** Growing evidence suggests a correlation between ulcerative colitis (UC) and immune markers. Pathogenesis of UC was not yet been clearly elucidated, and few researches on immune-related biomarkers published.

**1.2. Method:** We extracted gene expression profiles from GEO database, immune-related genes from the Immport database, and colon adenocarcinoma (COAD) data from TCGA and GTEx databases. Linear models for microarray data (LIMMA), weighted gene co-expression network analysis (WGCNA) and multiple algorithms were used to identify HUB genes. We performed gene expression analysis, principal component analysis (PCA) and receiver operating characteristic (ROC) analysis on the HUB genes to identify diagnostic ability of biomarkers. UC samples were stratified into high and low expression groups, and we conducted Correlation analysis and GSEA analysis between two groups. CIBERSORT algorithm was adopted to analyze the immune infiltration between UC and normal samples.

**1.3. Result:** We identified CXCL1, CCL20, and STAT1 as three key biomarkers related to UC immunity. Compared to normal samples, CXCL1, CCL20 and STAT1 were highly expressed in colon adenocarcinoma (COAD) samples. B cells naive, Plasma cells, T cells CD4 Memory activated, NK cells resting, Macrophages M0, Macrophages M1, Dendritic cells activated, Mast Cells activated, and Neutrophils were significantly higher in UC samples than normal samples. ( $p < 0.05$ ).

**1.4. Conclusion:** We successfully screened the immune-related gene biomarkers of UC, thus provided some innovative thinking for the diagnosis and related immunotherapy of UC patients.

### 2. Introduction

Ulcerative colitis (UC), as a global disease, displays an ascending worldwide incidence [1]. An epidemiological report revealed that incidence rate in some countries had exceeded 0.3% till 2018 and was still increasing [2]. Being a chronic inflammatory disease, UC makes involved the colon in any aspect from mucosal inflammation in the rectum to an extended proximal invasion in a continuous manner, with its characteristically alternating periods of relapse and remitting mucosal inflammation. Typical symptoms present as bloody diarrhoea, abdominal pain, faecal urgency, and tenesmus [3, 4]. The onset of UC peaks between the ages of 30 and 40 [5].

The pathogenesis of UC is multifactorial, including genetic predisposition, epithelial barrier defects, dysregulated immune responses, and environmental factors. Gastrointestinal tract (GI tract) plays a paramount part in maintaining immune homeostasis. The maintenance of homeostasis in the intestinal mucosa requires the stable activity of innate and adaptive immune cells coordinating. Mucosal barrier defect is correlating to UC, once the delicate balance between tolerance and inflammation of the gastrointestinal immune system is broken, a sustained and uninhibited inflammatory response will be triggered by the gut microbiota [6, 7].

Chronic ulcerative colitis exposes individuals to an increased possibility of developing colorectal cancer [8, 9]. As indicated in

some epidemiological data, inflammation, together with distinct arms of the host immune system, contributes greatly to tumorigenesis [10, 11]. Inflammatory environment is of great importance to the pathogenesis of colitis-associated cancer (CAC) patients, and it promotes the growth and development of CAC and affects its metastasis. Recent studies have shown that evading immune destruction, reprogramming of energy metabolism, gene mutation and oncogenic inflammation have become new hallmarks of cancer. Those components of the immune system involved in tumorigenesis and tumour progression have been proved to be key factors for cancer [11, 12].

However, with the pathogenesis of UC not yet been clearly elucidated, and especially, with few researches on immune-related biomarkers published, it emerges as a pressing issue to identify potential tissue biomarkers for the diagnosis or treatment of UC and CAC. In recent years, the rapid progress made in microarray technology and high-throughput sequencing technology has provided a platform for us to identify key genetic factors and biomarkers applied to the diagnosis, treatment and prognosis of diseases [13]. WGCNA has increasingly been used to analyze large, high-dimensional datasets, therefore can be commonly applied in identifying candidate biomarkers or therapeutic targets for diseases [14]. In this study, we worked on WGCNA and the immune-related genes from the ImmPort database using the five microarray datasets (GSE87473 GSE75214, GSE59071, GSE3629, GSE37283) in Gene Expression Omnibus (GEO) database. Furthermore, we analyzed the immune infiltration in UC samples via CIBERSORT algorithm to identify its differential genes and key biomarkers, thus to offer a target benefitting the diagnosis and treatment of UC.

## 2. Material and Methods

### 2.1. Data Sources and Processing

A summary of our flow chart are described (Figure 1). Gene expression profile including GSE87473, GSE75214, GSE59071, GSE3629, GSE37283 (Table 1) were downloaded from the Gene Expression Omnibus (GEO, <https://www.ncbi.nlm.nih.gov/geo/>) database. The data was collected between August 04 and August 30, 2020. GSE87473, GSE75214 were chosen as training datasets. GSE59071 was chosen as validation dataset to verify the results from training datasets. We downloaded platform and annotation files and converted the expression spectrum from the probe level to the corresponding gene symbol according to annotation

files. Batch effects were adjusted for GSE87473 and GSE75214 in training dataset using "SVA" (version 3.34.0) R package [15]. Subsequently, we used "limma" (version, 3.42.2) R package (<http://www.bioconductor.org/packages/release/bioc/html/limma.html>) for overall data correction, and if a gene corresponded to multiple lines, we would take the average. Genes with an expression rate of 0 in samples were deleted [16].

### 2.2 Identification of DEGs

By comparing expression levels between normal colon tissue and UC tissue, DEG was identified using a linear model "limma" (version 3.42.2) R package based on microarray data from Bioconductor. The adjusted  $p < 0.05$  and  $|\log_{2}FC| > 1$  were set as cutoff values, under the premise of which we drew the heatmap and volcano map of DEGs using "pheatmap" (version 1.0.12) and "ggplot2" (version 3.3.2) R software package.

### 2.3. WGCNA Construction

Weighted gene co-expression network analysis (WGCNA) is a systems biology method. It can be used to describe the correlation patterns among genes, identify network modules of highly correlated genes, relate these gene network modules to each other and to external sample traits, and identifying candidate biomarkers or therapeutic targets [14]. In this study, "WGCNA" (version 1.69) R software package was used in constructing the co-expression networks of the training dataset. The analysis process is as follows: (1) Construct a gene co-expression network. Pearson correlation coefficients were calculated for all genes in the training dataset to construct the gene co-expression networks. (2) Select "Soft" thresholds using scale-free topological criteria. Herein, we set  $\beta = 11$  (scale  $R^2 = 0.815$ ) to construct the scale-free networks, emphasizing the strong correlation between genes and penalized the weak [17]. (3) Identify modules. The information on the adjacency between 2 nodes was converted into a topological overlap measure (TOM) that can measure the connectivity of the gene network, and dissimilarity based on TOM. The minimum genome size of the gene treemap was 150, and the genes with similar expression profiles in the training data set were divided into different modules using hierarchical clustering and Dynamic Tree Cut [14]. (4) Module clustering. After the determination of gene modules, feature vectors of each module were calculated in sequence, followed by clustering of the modules. Neighboring modules were merged into new ones, and the height was set to 0.1 [18].

**Table 1:** Details about the data sets used in this study.

Patient data	Normal	UC	UC-Ca	Platform	Reference
GSE87473	21	106	-	Affymetrix HT HG-U133+ PM Array Plate	PMID: 29401083
GSE75214	22	97	-	Affymetrix Human Gene 1.0 ST Array	PMID: 28885228
GSE59071	11	97		Affymetrix Human Gene 1.0 ST Array	PMID: 26313692
GSE3629	-	43	10	Affymetrix Human Genome U133 Plus 2.0 Array	PMID: 17255260
GSE37283	5	4	11	Affymetrix HT HG-U133+ PM Array Plate	PMID: 23945234

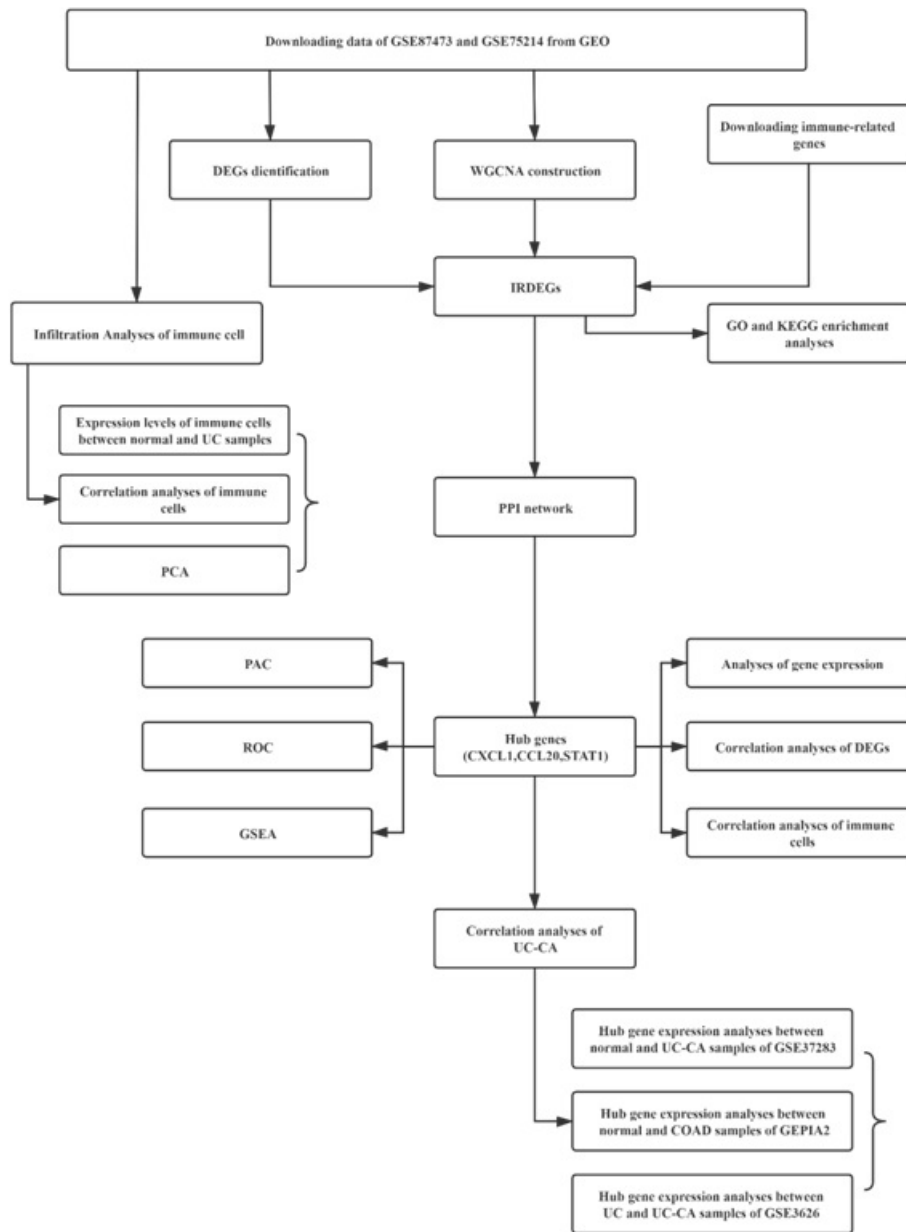


**Figure 1.** Flow chart of the whole procedures.

## 2.4. Identification and Analysis of Immune-related Differently Expressed Genes (IRDEGs)

Module Eigengene (ME) is reckoned as the uppermost major component in Principal Component Analysis (PCA) of each module, suggesting that within a given module, expression patterns of all genes can be summarized into a single characteristic expression profile. Key modules (green modules) were identified through the correlation between UC and ME, and genes in the green modules all had a high Pearson coefficient (Pearson coefficient = 0.61) [19].

In this study, 1793 immune-related genes were downloaded from ImmPort database (<https://import.niaid.nih.gov/>) for this study. The immune-related genes are comprised of 17 categories, including cytokines, interleukin, interferon, members of tumor necrosis

factor family, transforming growth factor $\beta$  family, chemokines, cytokine receptors, etc. DEGs, WGCNA identified immune-related genes. Key modules in the training dataset were intersected using the VennDiagram (version, 1.6.20) R software package. The ultimately overlapped genes was defined as IRDEGs [20]. In order to understand the relevant biological functions of IRDEGs, we conducted Gene ontological (GO) and Kyoto Encyclopedia of Genes and Genomes (KEGG) enrichment analysis upon the selected IRDEGs through cluster Profiler (version 3.14.3).

## 2.5. Screening of HUB Genes

STRING (<https://string-db.org/>) is a website tool to predict protein-protein interactions through algorithms [21], by the use of which a PPI network associated with IRGDEGs was built (confidence level

0.4). Cytoscape is an open source software project and used to integrate biomolecular interaction networks with high-throughput expression data and other molecular states into a unified conceptual framework [22]. “cytoHubba”, a molecular-complexity-detecting Cytoscape (version 3.7.2) plugin, was applied in screening the core genes of PPI network [23]. We defined HUB genes as the top 3 genes in the PPI network ranked by “degree”.

## 2.6. Analysis and Verification of HUB Genes

To understand whether hub genes differentiate between normal samples and UC samples, we performed Wilcoxon test on each single hub gene in training and validation dataset. The “beeswarm” (version 0.2.3) R package was subsequently used to draw boxplots of difference. According to hub genes’ varied expression levels of the samples in the training dataset were divided into high and low expression groups, and correlation analysis between the two groups was carried out. To study the significant change between the high and low expression groups, we conducted gene set enrichment analysis (GSEA) between the two genomes using GSEA package (version, 4.1.0, <https://www.gsea-msigdb.org/gsea/index.jsp>) [24]. Biological processes involved in this study depended on usage of the MSigDB marker genesets (c2.cp.kegg.v7.0.symbols.gmt).

To verify the correlation between HUB gene and UC, we used R software package “pROC (version : 1.16.2)” to draw receiver operating characteristic (ROC) curve of the verification dataset. If the area under ROC curve (AUC) > 0.7, the very HUB gene can be proved to distinguish between normal samples and UC samples. Principal Components Analysis (PCA) was applied to reduce the false association to the greatest extent while the ability to detect the true association was maximized, thus further proving the capability of HUB genes in securely differentiating the normal sample and the UC sample [25]. We chose COAD data in TCGA and GTEx databases from Gene Expression Profiling Interactive Analysis (GEPIA2) database (<http://gepia2.cancer-pku.cn>) [26], and GSE3629, GSE37283 datasets to testify the HUB genes’ correlation with UC - related colon cancer (UC-CA), as well as it with colorectal cancer.

Immunohistochemical method was used to detect the protein expression of hub gene in normal samples and UC samples. The immunohistochemical procedure is as follows: paraffin section dewaxing. Antigen repair: microwave heating for antigen repair. After hydration, PBS washing removed endogenous peroxidase. Endogenous peroxidase activity was blocked using a blocking solution (Biyuntian Biotechnology Co., Shanghai, China). The primary antibody (dilution ratio: 1:1000) was covered with Parafilm membrane and incubated overnight at 4°C, then washed for 3 times. The secondary antibody (dilution ratio: 1:50) was covered with Parafilm membrane and incubated at room temperature for 20min,

then washed for 3 times. Tri-antibody: Drop 100µL streptavidin labeled with horseradish peroxidase, cover with Parafilm and incubate at room temperature for 20min, then wash for 3 times. The DAB chromogenic solution developed for about 5min. Hematoxylin redyeing, dehydration, film sealing, microscopic examination, photography.

## 2.7. Analysis of immune Cell infiltration

We used CIBERSORT, a popular algorithm for predicting immune cell infiltration of fresh, frozen, and fixed tissues (solid tumors included), to understand infiltration of immune cells in distinct risk populations. CIBERSORT performs deconvolution algorithms on samples, using support vector regression for every cell type [27]. For each sample, CIBERSORT is able to infer the relative proportions of 22 types of infiltrating immune cells, including T cells, B cells, NK cells, eosinophils, plasma cells, macrophages, dendritic cells, neutrophils, etc. The relative proportion of infiltrating immune cells in each sample was calculated using the R package (CIBERSORT R Script version, 1.03). To observe the different abundance of each immune cell type between the normal and UC groups directly, correlation analysis was performed using “Vio-plot” (version 0.3.5) and the results were visualized. Then, correlation analysis was also done to determine what’s going on between hub gene expression level and immune cell content.

## 2.8. Statistical Analysis

All the statistical tests were performed depending on R language software (version 3.6.1, <https://www.r-project.org/>) and SPSS software (SPSS version 22, SPSS). For all the tests,  $p < 0.05$  was considered statistically significant.

## 3. Results

### 3.1. Identification of DEGs

After data correction, gene annotation, and removal of batch effects of GSE87473 and GSE75214 datasets, we obtained training dataset’s expression matrix, including 243 samples (43 normal samples, 203 UC samples) and 16,158 genes. Finally, 568 DEGs were detected (315 increased, 253 decreased) (Figure 2A,B) for subsequent analysis.

### 3.2. Construction of WGCNA and Identification of Key Modules

We established a WGCNA for the training dataset. A soft threshold  $\beta = 11$  was set to construct a scale-free network (Figure 2C) and gene-level cluster tree (Figure 2D). Then 7 modules were identified and colors were assigned to each module (Figure 2E). The correlation between the green module and UC tissue was higher than that of the other 6 modules ( $r = 0.61$ ,  $p = 3e-22$ ) (Figure 2F,G). All 478 genes in the green module were selected to further analysis.

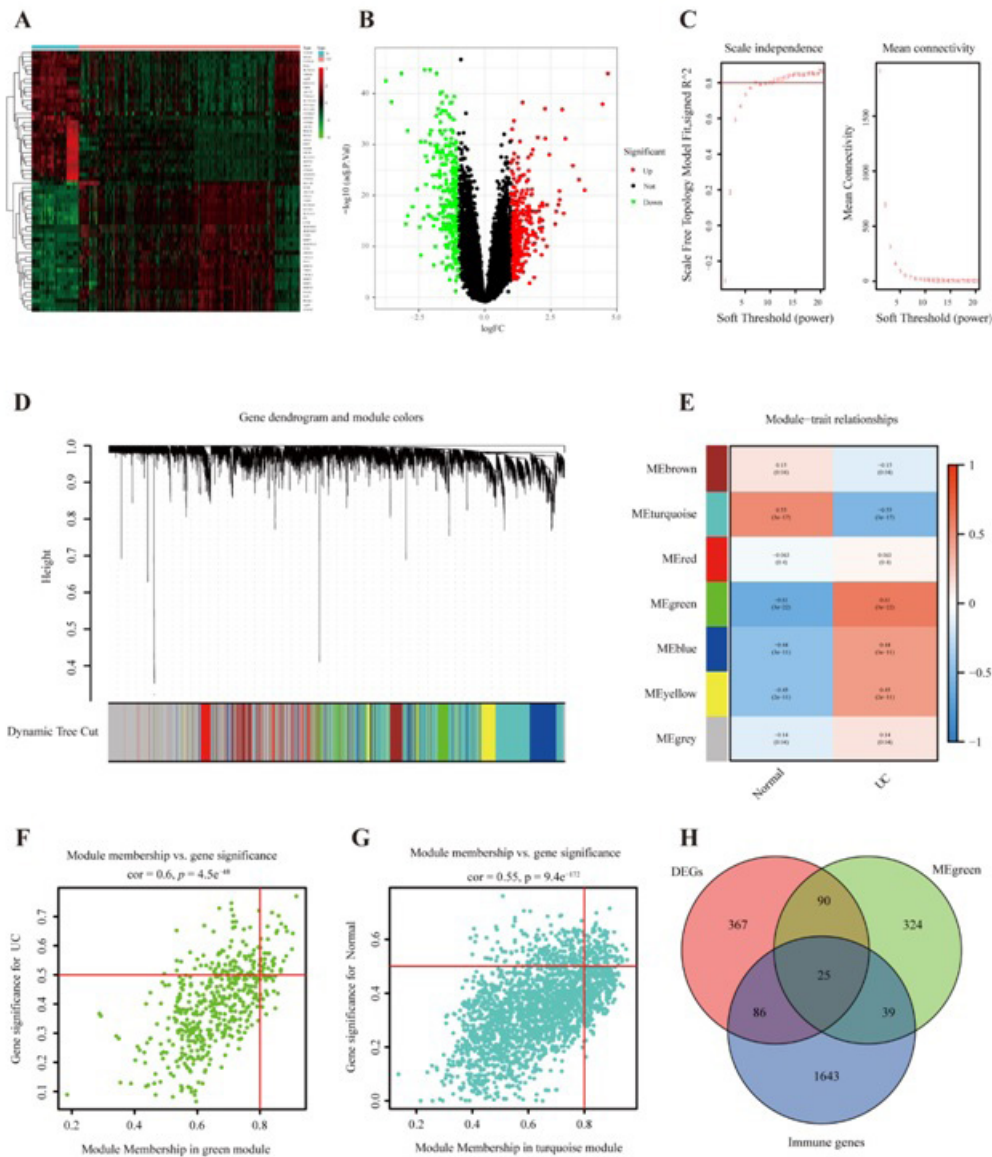


**Figure 2.** Heatmaps and volcano plots of differentially expressed genes between the normal and UC samples in the training dataset. **(A)** The heatmap of the differentially expressed genes in UC samples (all of the up-regulated and down-regulated genes). **(B)** The volcano plot of the differentially expressed genes in UC samples ( adjusted p-value < 0.05 and | log2FC| > 1 ). The weighted correlation network analysis (WGCNA) based on the training dataset. **(C)** Scale-free fitting index ( $\beta$ ) of soft threshold efficacy ( $\beta = 11$  (scale  $R^2 = 0.815$ )), mean connectivity analysis of soft threshold power based on gene hierarchy cluster tree of 1-TOM matrix. **(D)** Construction of a weighted gene co-expression network module based on dynamic branching shear method for training data sets, **(E)** The heatmap of correlation between module epigenes and clinical features (normal and UC). **(F)** The green modules in the most significant positive correlation with UC samples (the abscissa represents the correlation between genes and modules, and the ordinate represents the clinical correlation between genes and UC samples). **(G)** The blue modules in the most significant positive correlation with normal samples (the abscissa represents the correlation between genes and modules, and the ordinate represents the clinical correlation between genes and normal samples). **(H)** The Venn diagram of DEGs, key modules in the co-expression network and immune-related genes, and there are 25 immune-related differentially expressed genes (IRDEGs) .

**Abbreviation:** UC: Ulcerative Colitis, TOM: Topological Overlap Measure; DEGs: Differentially Expressed Genes

### 3.3. Identification and Functional Annotation of Immune-Related Differently Expressed Genes (IRDEGs)

We took the intersection of the 1,793 immune-related genes downloaded from the ImmPort database, 568 DEGs from the training dataset and 478 genes from the green module identified in WGCNA. Finally, a total of 25 overlapping genes were chosen as (IRDEGs) for subsequent analysis (Table 2) (Figure 2H). GO and KEGG enrichment analyses were conducted on these 25 overlapping genes, thus the cellular components, molecular functions, biological processes, and related biological pathways involved in IRDEGs can be determined. GO functional enrichment analysis showed such IRDEGs related biological processes (BP) as antimicrobial humoral response, humoral immune response, cell reaction to chemokines, antimicrobial peptide-mediated antimicrobial humoral immune response and other processes. The cell composition (CC) involved roughly including zymogen granule, secretory

granule cavity, cytoplasmic vesicle cavity, cystic space, etc. The molecular function (MF) involving chemokine receptor binding, chemokine activity, G protein-coupled receptor binding, cytokine activity, etc. (Table S1) (Figure 3C) KEGG pathway showed IRDEGs-related pathways mainly including chemokine signaling pathways, viral protein's interaction with cytokines and cytokine receptors, IL - 17 signaling pathways, cytokine-cytokine- receptor interaction, tumor necrosis factor signaling pathways, etc. (Table S2) (Figure 3A,B)

### 3.4 Screening of HUB genes

PPI network related to the 25 IRDEGs was constructed by STRING (Figure 3D). We obtained the top 15 genes ranked highest in the PPI network from Cytoscape (cytohubba plugin ) (Figure 3E). In this study, the most highly ranked 3 genes in the PPI network were seen as HUB genes (Figure 3F), including chemokine (CXC motif) ligand 1(CXCL1), chemokine (CC motif) ligand 20(CCL20), signal transduction and transcriptional activator 1(STAT1).

**Table 2:** Model information about IRDEGs.

IRDEGs	Full name	Immune processes
DUOX2	C-X-C motif chemokine ligand 11	Antimicrobials
LCN2	lactritin	Cytokines
PI3	placental growth factor	Cytokines
CXCL1	C-C motif chemokine ligand 4 like 2	Antimicrobials
S100A11	ribonuclease A family member 2	Cytokines
S100P	S100 calcium binding protein A6	Cytokines
NFKBIZ	neudesin neurotrophic factor	Cytokines
STAT1	somatostatin	Cytokines
PLAUR	plasminogen activator, urokinase	Cytokines
ADM	adrenomedullin	Cytokines
CXCL2	C-X-C motif chemokine ligand 12	Antimicrobials
LYN	latent transforming growth factor beta binding protein 4	Cytokines
NOS2	cellular communication network factor 3	Cytokines
AREG	amphiregulin	Cytokines
OSMR	endonuclease, poly(U) specific	Cytokines
IDO1	islet amyloid polypeptide	Cytokines
PLA2G2A	placental growth factor	Cytokines
CXCL3	C-X-C motif chemokine ligand 12	Antimicrobials
CXCL11	C-C motif chemokine ligand 4 like 2	Antimicrobials
CCL20	C-C motif chemokine ligand 20	Antimicrobials
CTSE	C-C motif chemokine ligand 4 like 2	Antimicrobials
CXCL9	C-X-C motif chemokine ligand 12	Antimicrobials
DMBT1	C-X-C motif chemokine ligand 11	Antimicrobials
CXCL10	C-C motif chemokine ligand 4 like 2	Antimicrobials
REG1A	regenerating family member 1 alpha	Cytokines

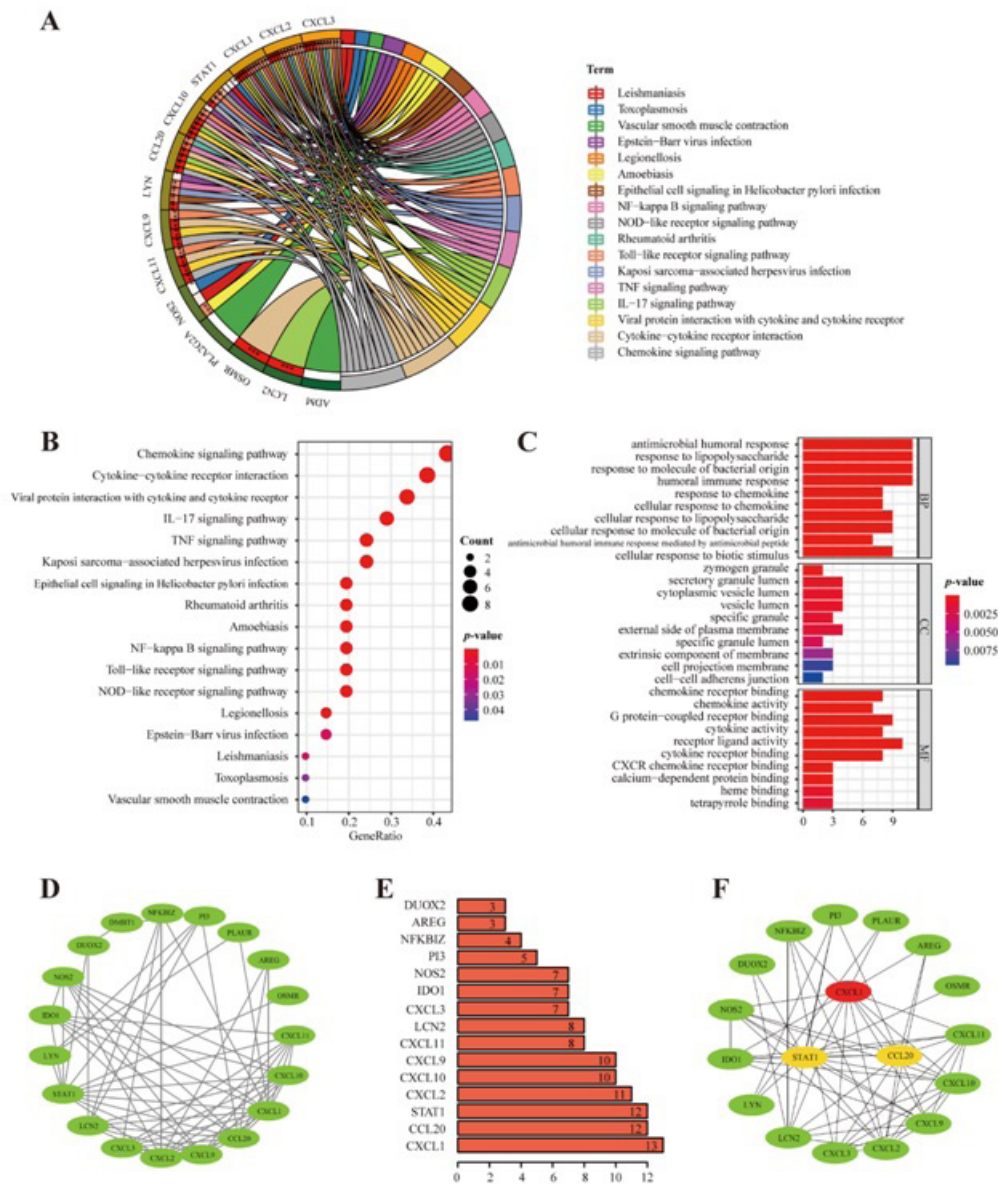


**Figure 3. (A)** Enrichment analysis results of the IRDEGs based on Kyoto Encyclopedia of Genes and Genomes (KEGG). **(B)** Gene ontological (GO) enrichment analysis results of the IRDEGs. **(C)** "GeneRatio" is the percentage of the total number of genes that differ in the given KEGG term. **(D)** The PPI network of IRDEGs using Cytoscape. **(E)** The most highly scored 15 genes in the PPI network of IRDEGs (using the degree algorithm in the cytohubba plugin of Cytoscape). **(F)** The 3 HUB genes in the PPI network of IRDEGs (CXCL1, CCL20, STAT1).

**Abbreviation:** UC: Ulcerative Colitis; IRDE: Immune-Related Differential Gene; GO: Gene Ontology; KEGG: Kyoto Encyclopedia of Genes and Genomics.

### 3.5. Analysis and Verification of CXCL1, CCL20 and STAT1

The expression of HUB genes in UC samples was more significant in both the training and verification dataset. (Figure 4A,B) We divided the training dataset into highly or lowly expressed according to the expression value of every single HUB gene (compared with the normal samples). The correlation analysis of the top 20 genes with the largest intergroup difference was carried out, as shown in (Figure 4C), in which red stands for the positive correlation of the two differential genes, while green represents the negative correlation.

GSEA analysis was performed to explore further KEGG pathway change between high-low expression groups (Table S3). CXCL1 expression were significantly enriched in butanoate metabolism, toll like receptor signaling pathway, cytokine-cytokine receptor interaction, CCL20 expression were significantly enriched in apoptosis, p53 signaling pathway, pathogenic escherichia coli infection, STAT1 expression were significantly enriched in antigen processing and presentation, chemokine signaling pathway, proximal tubule bicarbonate reclamation were those mostly affected. (Figure 5A).

According to the ROC curve plotted upon the validation dataset, HUB genes (CXCL1(AUG=94.4705),CCL20(AUG=92.8772)) and STAT1(AUG=92.3149) can be identified in strongly differentiation between normal samples and UC samples (Figure 5C). Through PCA analysis towards both the training and the validation datasets, it was clear that significant group bias clustering and individual differences were informed between the normal samples and

UC samples regarding HUB gene expression (Figure 5F).

Immunohistochemistry (IHC) was performed to detect the expression of CXCL1, CCL20, and STAT1 proteins in UC tissues and their corresponding surgical margin tissues, and we found that the expression of CXCL1, CCL20, and STAT1 proteins in UC tissues was higher than that in their corresponding surgical margin tissues (Figure 6A).

**Table 3:** GO analysis.

term.id	ontology	term.name	p.adjust
GO:0019730	BP	antimicrobial humoral response	2.45E-15
GO:0032496	BP	response to lipopolysaccharide	6.74E-11
GO:0002237	BP	response to molecule of bacterial origin	6.74E-11
GO:0006959	BP	humoral immune response	6.74E-11
GO:1990868	BP	response to chemokine	6.74E-11
GO:1990869	BP	cellular response to chemokine	6.74E-11
GO:0071222	BP	cellular response to lipopolysaccharide	4.96E-10
GO:0071219	BP	cellular response to molecule of bacterial origin	5.34E-10
GO:0061844	BP	antimicrobial humoral immune response mediated by antimicrobial peptide	5.34E-10
GO:0071216	BP	cellular response to biotic stimulus	1.23E-09
GO:0070098	BP	chemokine-mediated signaling pathway	1.68E-09
GO:0030593	BP	neutrophil chemotaxis	5.08E-09
GO:1990266	BP	neutrophil migration	1.15E-08
GO:0071621	BP	granulocyte chemotaxis	1.39E-08
GO:0097529	BP	myeloid leukocyte migration	1.39E-08
GO:0030595	BP	leukocyte chemotaxis	2.18E-08
GO:0097530	BP	granulocyte migration	3.09E-08
GO:0060326	BP	cell chemotaxis	2.16E-07
GO:0050900	BP	leukocyte migration	9.54E-06
GO:0009615	BP	response to virus	1.84E-04
GO:0051279	BP	regulation of release of sequestered calcium ion into cytosol	1.97E-04
GO:0010522	BP	regulation of calcium ion transport into cytosol	4.49E-04
GO:0019932	BP	second-messenger-mediated signaling	8.55E-04
GO:0051281	BP	positive regulation of release of sequestered calcium ion into cytosol	8.55E-04
GO:0051209	BP	release of sequestered calcium ion into cytosol	8.55E-04
GO:0051283	BP	negative regulation of sequestering of calcium ion	8.76E-04
GO:0051282	BP	regulation of sequestering of calcium ion	8.97E-04
GO:0051208	BP	sequestering of calcium ion	9.48E-04
GO:0055074	BP	calcium ion homeostasis	1.03E-03
GO:0007189	BP	adenylate cyclase-activating G protein-coupled receptor signaling pathway	1.10E-03
GO:0097553	BP	calcium ion transmembrane import into cytosol	1.10E-03
GO:0050727	BP	regulation of inflammatory response	1.10E-03
GO:1903169	BP	regulation of calcium ion transmembrane transport	1.40E-03
GO:0050729	BP	positive regulation of inflammatory response	1.43E-03
GO:0010524	BP	positive regulation of calcium ion transport into cytosol	1.46E-03
GO:0060402	BP	calcium ion transport into cytosol	1.53E-03
GO:0007204	BP	positive regulation of cytosolic calcium ion concentration	1.55E-03
GO:0032103	BP	positive regulation of response to external stimulus	1.61E-03
GO:0042742	BP	defense response to bacterium	1.69E-03
GO:0051235	BP	maintenance of location	1.69E-03



GO:0060401	BP	cytosolic calcium ion transport	1.83E-03
GO:0048247	BP	lymphocyte chemotaxis	2.03E-03
GO:0002548	BP	monocyte chemotaxis	2.03E-03
GO:0072678	BP	T cell migration	2.03E-03
GO:0051480	BP	regulation of cytosolic calcium ion concentration	2.18E-03
GO:0019933	BP	cAMP-mediated signaling	2.31E-03
GO:1904427	BP	positive regulation of calcium ion transmembrane transport	2.47E-03
GO:0002532	BP	production of molecular mediator involved in inflammatory response	2.52E-03
GO:0019935	BP	cyclic-nucleotide-mediated signaling	3.71E-03
GO:0007188	BP	adenylate cyclase-modulating G protein-coupled receptor signaling pathway	4.04E-03
GO:0071674	BP	mononuclear cell migration	4.60E-03
GO:0043434	BP	response to peptide hormone	4.79E-03
GO:0051607	BP	defense response to virus	5.06E-03
GO:0051591	BP	response to cAMP	5.41E-03
GO:0006874	BP	cellular calcium ion homeostasis	5.68E-03
GO:0051924	BP	regulation of calcium ion transport	6.13E-03
GO:0007187	BP	G protein-coupled receptor signaling pathway, coupled to cyclic nucleotide second messenger	6.21E-03
GO:1901739	BP	regulation of myoblast fusion	6.23E-03
GO:0043312	BP	neutrophil degranulation	6.89E-03
GO:0002283	BP	neutrophil activation involved in immune response	6.97E-03
GO:0072676	BP	lymphocyte migration	7.07E-03
GO:0072503	BP	cellular divalent inorganic cation homeostasis	7.07E-03
GO:0042119	BP	neutrophil activation	7.13E-03
GO:0002446	BP	neutrophil mediated immunity	7.13E-03
GO:0031667	BP	response to nutrient levels	7.13E-03
GO:0002507	BP	tolerance induction	7.68E-03
GO:0090025	BP	regulation of monocyte chemotaxis	7.68E-03
GO:0051928	BP	positive regulation of calcium ion transport	8.63E-03
GO:0010818	BP	T cell chemotaxis	9.24E-03
GO:2000108	BP	positive regulation of leukocyte apoptotic process	9.24E-03
GO:0060142	BP	regulation of syncytium formation by plasma membrane fusion	9.78E-03
GO:0046683	BP	response to organophosphorus	1.05E-02
GO:0070588	BP	calcium ion transmembrane transport	1.06E-02
GO:2000406	BP	positive regulation of T cell migration	1.07E-02
GO:1904064	BP	positive regulation of cation transmembrane transport	1.24E-02
GO:0042542	BP	response to hydrogen peroxide	1.27E-02
GO:0061041	BP	regulation of wound healing	1.30E-02
GO:0014074	BP	response to purine-containing compound	1.31E-02
GO:1904062	BP	regulation of cation transmembrane transport	1.32E-02
GO:0010742	BP	macrophage derived foam cell differentiation	1.32E-02
GO:0090077	BP	foam cell differentiation	1.32E-02
GO:2000403	BP	positive regulation of lymphocyte migration	1.38E-02
GO:0034767	BP	positive regulation of ion transmembrane transport	1.41E-02
GO:0007520	BP	myoblast fusion	1.65E-02
GO:2000404	BP	regulation of T cell migration	1.88E-02
GO:0032309	BP	icosanoid secretion	1.94E-02
GO:1903034	BP	regulation of response to wounding	1.96E-02
GO:0071675	BP	regulation of mononuclear cell migration	1.96E-02
GO:0071346	BP	cellular response to interferon-gamma	1.96E-02

GO:0010959	BP	regulation of metal ion transport	1.96E-02
GO:0045646	BP	regulation of erythrocyte differentiation	2.00E-02
GO:0002534	BP	cytokine production involved in inflammatory response	2.11E-02
GO:0071715	BP	icosanoid transport	2.11E-02
GO:1901571	BP	fatty acid derivative transport	2.11E-02
GO:0009409	BP	response to cold	2.15E-02
GO:0014009	BP	glial cell proliferation	2.15E-02
GO:0002685	BP	regulation of leukocyte migration	2.32E-02
GO:0045661	BP	regulation of myoblast differentiation	2.33E-02
GO:0070228	BP	regulation of lymphocyte apoptotic process	2.33E-02
GO:0034341	BP	response to interferon-gamma	2.34E-02
GO:0006816	BP	calcium ion transport	2.47E-02
GO:0034764	BP	positive regulation of transmembrane transport	2.47E-02
GO:0000768	BP	syncytium formation by plasma membrane fusion	2.48E-02
GO:0140253	BP	cell-cell fusion	2.48E-02
GO:0006949	BP	syncytium formation	2.63E-02
GO:0006979	BP	response to oxidative stress	2.72E-02
GO:0010830	BP	regulation of myotube differentiation	2.94E-02
GO:2000401	BP	regulation of lymphocyte migration	3.01E-02
GO:0000302	BP	response to reactive oxygen species	3.32E-02
GO:0034765	BP	regulation of ion transmembrane transport	3.33E-02
GO:0070838	BP	divalent metal ion transport	3.33E-02
GO:0072511	BP	divalent inorganic cation transport	3.44E-02
GO:0070227	BP	lymphocyte apoptotic process	3.44E-02
GO:0009266	BP	response to temperature stimulus	3.61E-02
GO:0006801	BP	superoxide metabolic process	3.67E-02
GO:0031100	BP	animal organ regeneration	3.67E-02
GO:0032945	BP	negative regulation of mononuclear cell proliferation	3.67E-02
GO:0050672	BP	negative regulation of lymphocyte proliferation	3.67E-02
GO:0070664	BP	negative regulation of leukocyte proliferation	4.15E-02
GO:0030193	BP	regulation of blood coagulation	4.22E-02
GO:1900046	BP	regulation of hemostasis	4.28E-02
GO:2000106	BP	regulation of leukocyte apoptotic process	4.56E-02
GO:0032868	BP	response to insulin	4.56E-02
GO:0045445	BP	myoblast differentiation	4.56E-02
GO:0050818	BP	regulation of coagulation	4.56E-02
GO:0043270	BP	positive regulation of ion transport	4.61E-02
GO:0042058	BP	regulation of epidermal growth factor receptor signaling pathway	4.66E-02
GO:0042446	BP	hormone biosynthetic process	4.66E-02
GO:0050829	BP	defense response to Gram-negative bacterium	4.84E-02
GO:0071356	BP	cellular response to tumor necrosis factor	5.23E-02
GO:1901184	BP	regulation of ERBB signaling pathway	5.30E-02
GO:0070372	BP	regulation of ERK1 and ERK2 cascade	5.60E-02
GO:0015908	BP	fatty acid transport	5.66E-02
GO:1903037	BP	regulation of leukocyte cell-cell adhesion	5.72E-02
GO:0050830	BP	defense response to Gram-positive bacterium	6.00E-02
GO:0034612	BP	response to tumor necrosis factor	6.00E-02
GO:0046879	BP	hormone secretion	6.00E-02
GO:0050863	BP	regulation of T cell activation	6.07E-02
GO:0070371	BP	ERK1 and ERK2 cascade	6.15E-02

GO:0071887	BP	leukocyte apoptotic process	6.15E-02
GO:0071375	BP	cellular response to peptide hormone stimulus	6.23E-02
GO:1901606	BP	alpha-amino acid catabolic process	6.23E-02
GO:0009914	BP	hormone transport	6.23E-02
GO:0060562	BP	epithelial tube morphogenesis	6.23E-02
GO:0046677	BP	response to antibiotic	6.45E-02
GO:0014902	BP	myotube differentiation	6.80E-02
GO:0007159	BP	leukocyte cell-cell adhesion	6.90E-02
GO:0002688	BP	regulation of leukocyte chemotaxis	6.90E-02
GO:0030218	BP	erythrocyte differentiation	6.90E-02
GO:0051153	BP	regulation of striated muscle cell differentiation	7.20E-02
GO:0007173	BP	epidermal growth factor receptor signaling pathway	7.39E-02
GO:0034101	BP	erythrocyte homeostasis	7.65E-02
GO:1903409	BP	reactive oxygen species biosynthetic process	7.65E-02
GO:0001666	BP	response to hypoxia	7.79E-02
GO:0046717	BP	acid secretion	7.79E-02
GO:0009063	BP	cellular amino acid catabolic process	7.86E-02
GO:0002687	BP	positive regulation of leukocyte migration	8.00E-02
GO:0036293	BP	response to decreased oxygen levels	8.00E-02
GO:0006569	BP	tryptophan catabolic process	8.00E-02
GO:0031284	BP	positive regulation of guanylate cyclase activity	8.00E-02
GO:0034135	BP	regulation of toll-like receptor 2 signaling pathway	8.00E-02
GO:0042436	BP	indole-containing compound catabolic process	8.00E-02
GO:0046218	BP	indolalkylamine catabolic process	8.00E-02
GO:0060600	BP	dichotomous subdivision of an epithelial terminal unit	8.00E-02
GO:0071104	BP	response to interleukin-9	8.00E-02
GO:0072203	BP	cell proliferation involved in metanephros development	8.00E-02
GO:0097048	BP	dendritic cell apoptotic process	8.00E-02
GO:2000668	BP	regulation of dendritic cell apoptotic process	8.00E-02
GO:2001214	BP	positive regulation of vasculogenesis	8.00E-02
GO:0050678	BP	regulation of epithelial cell proliferation	8.08E-02
GO:0031346	BP	positive regulation of cell projection organization	8.08E-02
GO:0045765	BP	regulation of angiogenesis	8.08E-02
GO:0042692	BP	muscle cell differentiation	8.08E-02
GO:1901653	BP	cellular response to peptide	8.08E-02
GO:0034605	BP	cellular response to heat	8.08E-02
GO:0001821	BP	histamine secretion	8.08E-02
GO:0002517	BP	T cell tolerance induction	8.08E-02
GO:0046886	BP	positive regulation of hormone biosynthetic process	8.08E-02
GO:0070106	BP	interleukin-27-mediated signaling pathway	8.08E-02
GO:0070189	BP	kynurenine metabolic process	8.08E-02
GO:0070757	BP	interleukin-35-mediated signaling pathway	8.08E-02
GO:1901678	BP	iron coordination entity transport	8.08E-02
GO:1905245	BP	regulation of aspartic-type peptidase activity	8.08E-02
GO:2000318	BP	positive regulation of T-helper 17 type immune response	8.08E-02
GO:0070482	BP	response to oxygen levels	8.27E-02
GO:0038127	BP	ERBB signaling pathway	8.27E-02
GO:0003337	BP	mesenchymal to epithelial transition involved in metanephros morphogenesis	8.27E-02
GO:0006527	BP	arginine catabolic process	8.27E-02

GO:0006568	BP	tryptophan metabolic process	8.27E-02
GO:0006991	BP	response to sterol depletion	8.27E-02
GO:0031282	BP	regulation of guanylate cyclase activity	8.27E-02
GO:0042118	BP	endothelial cell activation	8.27E-02
GO:0051608	BP	histamine transport	8.27E-02
GO:0060368	BP	regulation of Fc receptor mediated stimulatory signaling pathway	8.27E-02
GO:0060670	BP	branching involved in labyrinthine layer morphogenesis	8.27E-02
GO:0022407	BP	regulation of cell-cell adhesion	8.27E-02
GO:0045834	BP	positive regulation of lipid metabolic process	8.27E-02
GO:0051250	BP	negative regulation of lymphocyte activation	8.27E-02
GO:0051384	BP	response to glucocorticoid	8.27E-02
GO:0002262	BP	myeloid cell homeostasis	8.33E-02
GO:0007494	BP	midgut development	8.40E-02
GO:0009635	BP	response to herbicide	8.40E-02
GO:0010838	BP	positive regulation of keratinocyte proliferation	8.40E-02
GO:0034374	BP	low-density lipoprotein particle remodeling	8.40E-02
GO:0043116	BP	negative regulation of vascular permeability	8.40E-02
GO:0060712	BP	spongiotrophoblast layer development	8.40E-02
GO:0061469	BP	regulation of type B pancreatic cell proliferation	8.40E-02
GO:0061478	BP	response to platelet aggregation inhibitor	8.40E-02
GO:0072182	BP	regulation of nephron tubule epithelial cell differentiation	8.40E-02
GO:0062013	BP	positive regulation of small molecule metabolic process	8.56E-02
GO:1901342	BP	regulation of vasculature development	8.66E-02
GO:0007259	BP	JAK-STAT cascade	8.66E-02
GO:0052548	BP	regulation of endopeptidase activity	8.66E-02
GO:0032310	BP	prostaglandin secretion	8.66E-02
GO:0051712	BP	positive regulation of killing of cells of other organism	8.66E-02
GO:0060397	BP	JAK-STAT cascade involved in growth hormone signaling pathway	8.66E-02
GO:0070234	BP	positive regulation of T cell apoptotic process	8.66E-02
GO:2001212	BP	regulation of vasculogenesis	8.66E-02
GO:0050673	BP	epithelial cell proliferation	8.83E-02
GO:0015718	BP	monocarboxylic acid transport	8.83E-02
GO:0031960	BP	response to corticosteroid	8.83E-02
GO:0017014	BP	protein nitrosylation	8.83E-02
GO:0018119	BP	peptidyl-cysteine S-nitrosylation	8.83E-02
GO:0032352	BP	positive regulation of hormone metabolic process	8.83E-02
GO:0034134	BP	toll-like receptor 2 signaling pathway	8.83E-02
GO:0051770	BP	positive regulation of nitric-oxide synthase biosynthetic process	8.83E-02
GO:0072075	BP	metanephric mesenchyme development	8.83E-02
GO:0072160	BP	nephron tubule epithelial cell differentiation	8.83E-02
GO:0072283	BP	metanephric renal vesicle morphogenesis	8.83E-02
GO:0035821	BP	modification of morphology or physiology of other organism	8.87E-02
GO:0097696	BP	STAT cascade	8.87E-02
GO:0002643	BP	regulation of tolerance induction	8.87E-02
GO:0002830	BP	positive regulation of type 2 immune response	8.87E-02
GO:0010566	BP	regulation of ketone biosynthetic process	8.87E-02
GO:0016540	BP	protein autoprocesing	8.87E-02
GO:0030889	BP	negative regulation of B cell proliferation	8.87E-02
GO:0042448	BP	progesterone metabolic process	8.87E-02

GO:0051238	BP	sequestering of metal ion	8.87E-02
GO:0045088	BP	regulation of innate immune response	8.87E-02
GO:0052547	BP	regulation of peptidase activity	8.87E-02
GO:0016525	BP	negative regulation of angiogenesis	8.87E-02
GO:0002031	BP	G protein-coupled receptor internalization	8.87E-02
GO:0006586	BP	indolalkylamine metabolic process	8.87E-02
GO:0006590	BP	thyroid hormone generation	8.87E-02
GO:0010744	BP	positive regulation of macrophage derived foam cell differentiation	8.87E-02
GO:0010819	BP	regulation of T cell chemotaxis	8.87E-02
GO:0015732	BP	prostaglandin transport	8.87E-02
GO:0036149	BP	phosphatidylinositol acyl-chain remodeling	8.87E-02
GO:0050665	BP	hydrogen peroxide biosynthetic process	8.87E-02
GO:0051709	BP	regulation of killing of cells of other organism	8.87E-02
GO:0090185	BP	negative regulation of kidney development	8.87E-02
GO:1905331	BP	negative regulation of morphogenesis of an epithelium	8.87E-02
GO:2001267	BP	regulation of cysteine-type endopeptidase activity involved in apoptotic signaling pathway	8.87E-02
GO:0002697	BP	regulation of immune effector process	8.87E-02
GO:0002695	BP	negative regulation of leukocyte activation	8.87E-02
GO:2000181	BP	negative regulation of blood vessel morphogenesis	8.87E-02
GO:0009408	BP	response to heat	8.87E-02
GO:0023061	BP	signal release	8.87E-02
GO:0042110	BP	T cell activation	8.87E-02
GO:0071347	BP	cellular response to interleukin-1	8.87E-02
GO:0002902	BP	regulation of B cell apoptotic process	8.87E-02
GO:0007221	BP	positive regulation of transcription of Notch receptor target	8.87E-02
GO:0010832	BP	negative regulation of myotube differentiation	8.87E-02
GO:0032693	BP	negative regulation of interleukin-10 production	8.87E-02
GO:0036148	BP	phosphatidylglycerol acyl-chain remodeling	8.87E-02
GO:0060749	BP	mammary gland alveolus development	8.87E-02
GO:0061377	BP	mammary gland lobule development	8.87E-02
GO:0070230	BP	positive regulation of lymphocyte apoptotic process	8.87E-02
GO:0070233	BP	negative regulation of T cell apoptotic process	8.87E-02
GO:0072077	BP	renal vesicle morphogenesis	8.87E-02
GO:0090026	BP	positive regulation of monocyte chemotaxis	8.87E-02
GO:0090330	BP	regulation of platelet aggregation	8.87E-02
GO:2000319	BP	regulation of T-helper 17 cell differentiation	8.87E-02
GO:1905330	BP	regulation of morphogenesis of an epithelium	8.89E-02
GO:0051147	BP	regulation of muscle cell differentiation	8.90E-02
GO:0008217	BP	regulation of blood pressure	8.90E-02
GO:0061138	BP	morphogenesis of a branching epithelium	8.90E-02
GO:1903706	BP	regulation of hemopoiesis	8.90E-02
GO:0002544	BP	chronic inflammatory response	8.90E-02
GO:0003159	BP	morphogenesis of an endothelium	8.90E-02
GO:0060231	BP	mesenchymal to epithelial transition	8.90E-02
GO:0060252	BP	positive regulation of glial cell proliferation	8.90E-02
GO:0061154	BP	endothelial tube morphogenesis	8.90E-02
GO:0072074	BP	kidney mesenchyme development	8.90E-02
GO:0072087	BP	renal vesicle development	8.90E-02

GO:1901741	BP	positive regulation of myoblast fusion	8.90E-02
GO:2000696	BP	regulation of epithelial cell differentiation involved in kidney development	8.90E-02
GO:1903708	BP	positive regulation of hemopoiesis	8.90E-02
GO:1901343	BP	negative regulation of vasculature development	8.99E-02
GO:0051249	BP	regulation of lymphocyte activation	8.99E-02
GO:0006525	BP	arginine metabolic process	8.99E-02
GO:0007620	BP	copulation	8.99E-02
GO:0034143	BP	regulation of toll-like receptor 4 signaling pathway	8.99E-02
GO:0035458	BP	cellular response to interferon-beta	8.99E-02
GO:0051767	BP	nitric-oxide synthase biosynthetic process	8.99E-02
GO:0051769	BP	regulation of nitric-oxide synthase biosynthetic process	8.99E-02
GO:0060602	BP	branch elongation of an epithelium	8.99E-02
GO:0072234	BP	metanephric nephron tubule development	8.99E-02
GO:1902993	BP	positive regulation of amyloid precursor protein catabolic process	8.99E-02
GO:0007565	BP	female pregnancy	9.07E-02
GO:0050731	BP	positive regulation of peptidyl-tyrosine phosphorylation	9.07E-02
GO:0002029	BP	desensitization of G protein-coupled receptor signaling pathway	9.07E-02
GO:0010893	BP	positive regulation of steroid biosynthetic process	9.07E-02
GO:0017000	BP	antibiotic biosynthetic process	9.07E-02
GO:0022401	BP	negative adaptation of signaling pathway	9.07E-02
GO:0036150	BP	phosphatidylserine acyl-chain remodeling	9.07E-02
GO:0042402	BP	cellular biogenic amine catabolic process	9.07E-02
GO:0042403	BP	thyroid hormone metabolic process	9.07E-02
GO:0060713	BP	labyrinthine layer morphogenesis	9.07E-02
GO:0072111	BP	cell proliferation involved in kidney development	9.07E-02
GO:2000316	BP	regulation of T-helper 17 type immune response	9.07E-02
GO:0001763	BP	morphogenesis of a branching structure	9.11E-02
GO:0002221	BP	pattern recognition receptor signaling pathway	9.11E-02
GO:0031099	BP	regeneration	9.11E-02
GO:0050866	BP	negative regulation of cell activation	9.11E-02
GO:0023058	BP	adaptation of signaling pathway	9.11E-02
GO:0031281	BP	positive regulation of cyclase activity	9.11E-02
GO:0032727	BP	positive regulation of interferon-alpha production	9.11E-02
GO:0035584	BP	calcium-mediated signaling using intracellular calcium source	9.11E-02
GO:0035809	BP	regulation of urine volume	9.11E-02
GO:0044342	BP	type B pancreatic cell proliferation	9.11E-02
GO:0045117	BP	azole transport	9.11E-02
GO:0045624	BP	positive regulation of T-helper cell differentiation	9.11E-02
GO:0045663	BP	positive regulation of myoblast differentiation	9.11E-02
GO:0006575	BP	cellular modified amino acid metabolic process	9.25E-02
GO:0050870	BP	positive regulation of T cell activation	9.25E-02
GO:0009310	BP	amine catabolic process	9.29E-02
GO:0051349	BP	positive regulation of lyase activity	9.29E-02
GO:0072170	BP	metanephric tubule development	9.29E-02
GO:0072215	BP	regulation of metanephros development	9.29E-02
GO:0072243	BP	metanephric nephron epithelium development	9.29E-02
GO:1903861	BP	positive regulation of dendrite extension	9.29E-02
GO:0050679	BP	positive regulation of epithelial cell proliferation	9.39E-02
GO:0070555	BP	response to interleukin-1	9.41E-02

GO:0050670	BP	regulation of lymphocyte proliferation	9.41E-02
GO:0032944	BP	regulation of mononuclear cell proliferation	9.41E-02
GO:0001783	BP	B cell apoptotic process	9.41E-02
GO:0002227	BP	innate immune response in mucosa	9.41E-02
GO:0042430	BP	indole-containing compound metabolic process	9.41E-02
GO:0042537	BP	benzene-containing compound metabolic process	9.41E-02
GO:0060396	BP	growth hormone receptor signaling pathway	9.41E-02
GO:0071677	BP	positive regulation of mononuclear cell migration	9.41E-02
GO:0009612	BP	response to mechanical stimulus	9.44E-02
GO:0002053	BP	positive regulation of mesenchymal cell proliferation	9.49E-02
GO:0034110	BP	regulation of homotypic cell-cell adhesion	9.49E-02
GO:0045662	BP	negative regulation of myoblast differentiation	9.49E-02
GO:0060330	BP	regulation of response to interferon-gamma	9.49E-02
GO:0060334	BP	regulation of interferon-gamma-mediated signaling pathway	9.49E-02
GO:0060444	BP	branching involved in mammary gland duct morphogenesis	9.49E-02
GO:0071378	BP	cellular response to growth hormone stimulus	9.49E-02
GO:0072202	BP	cell differentiation involved in metanephros development	9.49E-02
GO:0072273	BP	metanephric nephron morphogenesis	9.49E-02
GO:1903859	BP	regulation of dendrite extension	9.49E-02
GO:0070374	BP	positive regulation of ERK1 and ERK2 cascade	9.55E-02
GO:0002699	BP	positive regulation of immune effector process	9.56E-02
GO:0050920	BP	regulation of chemotaxis	9.56E-02
GO:1903039	BP	positive regulation of leukocyte cell-cell adhesion	9.56E-02
GO:0002230	BP	positive regulation of defense response to virus by host	9.56E-02
GO:0006700	BP	C21-steroid hormone biosynthetic process	9.56E-02
GO:0010460	BP	positive regulation of heart rate	9.56E-02
GO:0010996	BP	response to auditory stimulus	9.56E-02
GO:0036152	BP	phosphatidylethanolamine acyl-chain remodeling	9.56E-02
GO:0060669	BP	embryonic placenta morphogenesis	9.56E-02
GO:0072539	BP	T-helper 17 cell differentiation	9.56E-02
GO:0007584	BP	response to nutrient	9.58E-02
GO:0044706	BP	multi-multicellular organism process	9.63E-02
GO:0070663	BP	regulation of leukocyte proliferation	9.63E-02
GO:1901605	BP	alpha-amino acid metabolic process	9.63E-02
GO:0002026	BP	regulation of the force of heart contraction	9.63E-02
GO:0035902	BP	response to immobilization stress	9.63E-02
GO:0036151	BP	phosphatidylcholine acyl-chain remodeling	9.63E-02
GO:0046885	BP	regulation of hormone biosynthetic process	9.63E-02
GO:0060143	BP	positive regulation of syncytium formation by plasma membrane fusion	9.63E-02
GO:0072207	BP	metanephric epithelium development	9.63E-02
GO:1901623	BP	regulation of lymphocyte chemotaxis	9.63E-02
GO:0008209	BP	androgen metabolic process	9.75E-02
GO:0009065	BP	glutamine family amino acid catabolic process	9.75E-02
GO:0009074	BP	aromatic amino acid family catabolic process	9.75E-02
GO:0032647	BP	regulation of interferon-alpha production	9.75E-02
GO:0033598	BP	mammary gland epithelial cell proliferation	9.75E-02
GO:0034368	BP	protein-lipid complex remodeling	9.75E-02
GO:0034369	BP	plasma lipoprotein particle remodeling	9.75E-02
GO:0035456	BP	response to interferon-beta	9.75E-02
GO:0042730	BP	fibrinolysis	9.75E-02

GO:0007263	BP	nitric oxide mediated signal transduction	9.91E-02
GO:0034367	BP	protein-containing complex remodeling	9.91E-02
GO:0050855	BP	regulation of B cell receptor signaling pathway	9.91E-02
GO:0070102	BP	interleukin-6-mediated signaling pathway	9.91E-02
GO:0070229	BP	negative regulation of lymphocyte apoptotic process	9.91E-02
GO:0072538	BP	T-helper 17 type immune response	9.91E-02
GO:0072606	BP	interleukin-8 secretion	9.91E-02
GO:0042445	BP	hormone metabolic process	9.91E-02
GO:0060560	BP	developmental growth involved in morphogenesis	9.97E-02
GO:0001782	BP	B cell homeostasis	9.97E-02
GO:0002828	BP	regulation of type 2 immune response	9.97E-02
GO:0010743	BP	regulation of macrophage derived foam cell differentiation	9.97E-02
GO:0032607	BP	interferon-alpha production	9.97E-02
GO:0043372	BP	positive regulation of CD4-positive, alpha-beta T cell differentiation	9.97E-02
GO:0045940	BP	positive regulation of steroid metabolic process	9.97E-02
GO:0050869	BP	negative regulation of B cell activation	9.97E-02
GO:0090200	BP	positive regulation of release of cytochrome c from mitochondria	9.97E-02
GO:0097421	BP	liver regeneration	9.97E-02
GO:0050663	BP	cytokine secretion	9.99E-02
GO:0002675	BP	positive regulation of acute inflammatory response	9.99E-02
GO:0003401	BP	axis elongation	9.99E-02
GO:0006658	BP	phosphatidylserine metabolic process	9.99E-02
GO:0010543	BP	regulation of platelet activation	9.99E-02
GO:0043304	BP	regulation of mast cell degranulation	9.99E-02
GO:0043457	BP	regulation of cellular respiration	9.99E-02
GO:0045648	BP	positive regulation of erythrocyte differentiation	9.99E-02
GO:0045742	BP	positive regulation of epidermal growth factor receptor signaling pathway	9.99E-02
GO:0046471	BP	phosphatidylglycerol metabolic process	9.99E-02
GO:0050482	BP	arachidonic acid secretion	9.99E-02
GO:1903963	BP	arachidonate transport	9.99E-02
GO:0003338	BP	metanephros morphogenesis	1.02E-01
GO:0033006	BP	regulation of mast cell activation involved in immune response	1.02E-01
GO:0042744	BP	hydrogen peroxide catabolic process	1.02E-01
GO:0043552	BP	positive regulation of phosphatidylinositol 3-kinase activity	1.02E-01
GO:0070207	BP	protein homotrimerization	1.02E-01
GO:0048872	BP	homeostasis of number of cells	1.03E-01
GO:0097237	BP	cellular response to toxic substance	1.03E-01
GO:0042180	BP	cellular ketone metabolic process	1.03E-01
GO:0010464	BP	regulation of mesenchymal cell proliferation	1.03E-01
GO:0010837	BP	regulation of keratinocyte proliferation	1.03E-01
GO:0060603	BP	mammary gland duct morphogenesis	1.03E-01
GO:0070232	BP	regulation of T cell apoptotic process	1.03E-01
GO:1901186	BP	positive regulation of ERBB signaling pathway	1.03E-01
GO:0010951	BP	negative regulation of endopeptidase activity	1.04E-01
GO:0045637	BP	regulation of myeloid cell differentiation	1.04E-01
GO:0022409	BP	positive regulation of cell-cell adhesion	1.06E-01
GO:0050730	BP	regulation of peptidyl-tyrosine phosphorylation	1.06E-01
GO:0032735	BP	positive regulation of interleukin-12 production	1.06E-01
GO:0034142	BP	toll-like receptor 4 signaling pathway	1.06E-01
GO:0042092	BP	type 2 immune response	1.06E-01



GO:0045622	BP	regulation of T-helper cell differentiation	1.06E-01
GO:0060251	BP	regulation of glial cell proliferation	1.06E-01
GO:0097484	BP	dendrite extension	1.06E-01
GO:0110111	BP	negative regulation of animal organ morphogenesis	1.06E-01
GO:1902991	BP	regulation of amyloid precursor protein catabolic process	1.06E-01
GO:0002385	BP	mucosal immune response	1.08E-01
GO:0042554	BP	superoxide anion generation	1.08E-01
GO:0090218	BP	positive regulation of lipid kinase activity	1.08E-01
GO:2000516	BP	positive regulation of CD4-positive, alpha-beta T cell activation	1.08E-01
GO:0010466	BP	negative regulation of peptidase activity	1.09E-01
GO:0033280	BP	response to vitamin D	1.10E-01
GO:0038083	BP	peptidyl-tyrosine autophosphorylation	1.10E-01
GO:0043114	BP	regulation of vascular permeability	1.10E-01
GO:0050691	BP	regulation of defense response to virus by host	1.10E-01
GO:0031668	BP	cellular response to extracellular stimulus	1.11E-01
GO:0010831	BP	positive regulation of myotube differentiation	1.11E-01
GO:0032350	BP	regulation of hormone metabolic process	1.11E-01
GO:0060416	BP	response to growth hormone	1.11E-01
GO:1903523	BP	negative regulation of blood circulation	1.11E-01
GO:0042588	CC	zymogen granule	1.35E-02
GO:0034774	CC	secretory granule lumen	1.98E-02
GO:0060205	CC	cytoplasmic vesicle lumen	1.98E-02
GO:0031983	CC	vesicle lumen	1.98E-02
GO:0042581	CC	specific granule	2.05E-02
GO:0009897	CC	external side of plasma membrane	2.28E-02
GO:0035580	CC	specific granule lumen	3.86E-02
GO:0019898	CC	extrinsic component of membrane	7.25E-02
GO:0031253	CC	cell projection membrane	9.29E-02
GO:0005913	CC	cell-cell adherens junction	9.29E-02
GO:0042589	CC	zymogen granule membrane	1.13E-01
GO:0031252	CC	cell leading edge	1.13E-01
GO:0043020	CC	NADPH oxidase complex	1.39E-01
GO:0071437	CC	invadopodium	1.39E-01
GO:0099091	CC	postsynaptic specialization, intracellular component	1.64E-01
GO:0042629	CC	mast cell granule	1.64E-01
GO:0031528	CC	microvillus membrane	1.64E-01
GO:0032809	CC	neuronal cell body membrane	1.78E-01
GO:0044298	CC	cell body membrane	1.78E-01
GO:0008305	CC	integrin complex	1.87E-01
GO:0098636	CC	protein complex involved in cell adhesion	1.95E-01
GO:0032590	CC	dendrite membrane	2.17E-01
GO:0042379	MF	chemokine receptor binding	2.75E-12
GO:0008009	MF	chemokine activity	2.05E-11
GO:0001664	MF	G protein-coupled receptor binding	3.31E-09
GO:0005125	MF	cytokine activity	1.03E-08
GO:0048018	MF	receptor ligand activity	1.03E-08
GO:0005126	MF	cytokine receptor binding	6.65E-08
GO:0045236	MF	CXCR chemokine receptor binding	6.47E-06
GO:0048306	MF	calcium-dependent protein binding	1.18E-03
GO:0020037	MF	heme binding	1.09E-02
GO:0046906	MF	tetrapyrrole binding	1.21E-02

GO:0008083	MF	growth factor activity	1.53E-02
GO:0048020	MF	CCR chemokine receptor binding	1.54E-02
GO:0005539	MF	glycosaminoglycan binding	3.40E-02
GO:0050839	MF	cell adhesion molecule binding	3.91E-02
GO:0016651	MF	oxidoreductase activity, acting on NAD(P)H	7.34E-02
GO:0045296	MF	cadherin binding	7.63E-02
GO:0070851	MF	growth factor receptor binding	8.79E-02
GO:0050786	MF	RAGE receptor binding	8.79E-02
GO:0019903	MF	protein phosphatase binding	8.79E-02
GO:0016175	MF	superoxide-generating NADPH oxidase activity	8.79E-02
GO:0016653	MF	oxidoreductase activity, acting on NAD(P)H, heme protein as acceptor	8.79E-02
GO:0005161	MF	platelet-derived growth factor receptor binding	8.79E-02
GO:0044548	MF	S100 protein binding	8.79E-02
GO:0070492	MF	oligosaccharide binding	8.79E-02
GO:0010181	MF	FMN binding	8.79E-02
GO:0030280	MF	structural constituent of epidermis	8.79E-02
GO:0047498	MF	calcium-dependent phospholipase A2 activity	8.79E-02
GO:0008201	MF	heparin binding	8.79E-02
GO:0042834	MF	peptidoglycan binding	8.79E-02
GO:0050664	MF	oxidoreductase activity, acting on NAD(P)H, oxygen as acceptor	8.79E-02
GO:0098641	MF	cadherin binding involved in cell-cell adhesion	9.28E-02
GO:0019902	MF	phosphatase binding	9.28E-02
GO:0008329	MF	signaling pattern recognition receptor activity	9.28E-02
GO:0038187	MF	pattern recognition receptor activity	9.28E-02
GO:0051861	MF	glycolipid binding	9.28E-02
GO:0046625	MF	sphingolipid binding	9.67E-02
GO:0004190	MF	aspartic-type endopeptidase activity	9.67E-02
GO:0102567	MF	phospholipase A2 activity (consuming 1,2-dipalmitoylphosphatidylcholine)	9.67E-02
GO:0102568	MF	phospholipase A2 activity consuming 1,2-dioleoylphosphatidylethanolamine)	9.67E-02
GO:0043015	MF	gamma-tubulin binding	9.67E-02
GO:0070001	MF	aspartic-type peptidase activity	9.67E-02
GO:0016702	MF	oxidoreductase activity, acting on single donors with incorporation of molecular oxygen, incorporation of two atoms of oxygen	9.67E-02
GO:0046875	MF	ephrin receptor binding	9.67E-02
GO:0016701	MF	oxidoreductase activity, acting on single donors with incorporation of molecular oxygen	9.80E-02
GO:0035035	MF	histone acetyltransferase binding	9.92E-02
GO:0005164	MF	tumor necrosis factor receptor binding	1.03E-01
GO:0051721	MF	protein phosphatase 2A binding	1.03E-01
GO:0004623	MF	phospholipase A2 activity	1.03E-01
GO:0005154	MF	epidermal growth factor receptor binding	1.03E-01
GO:0000979	MF	RNA polymerase II core promoter sequence-specific DNA binding	1.04E-01
GO:1901681	MF	sulfur compound binding	1.05E-01

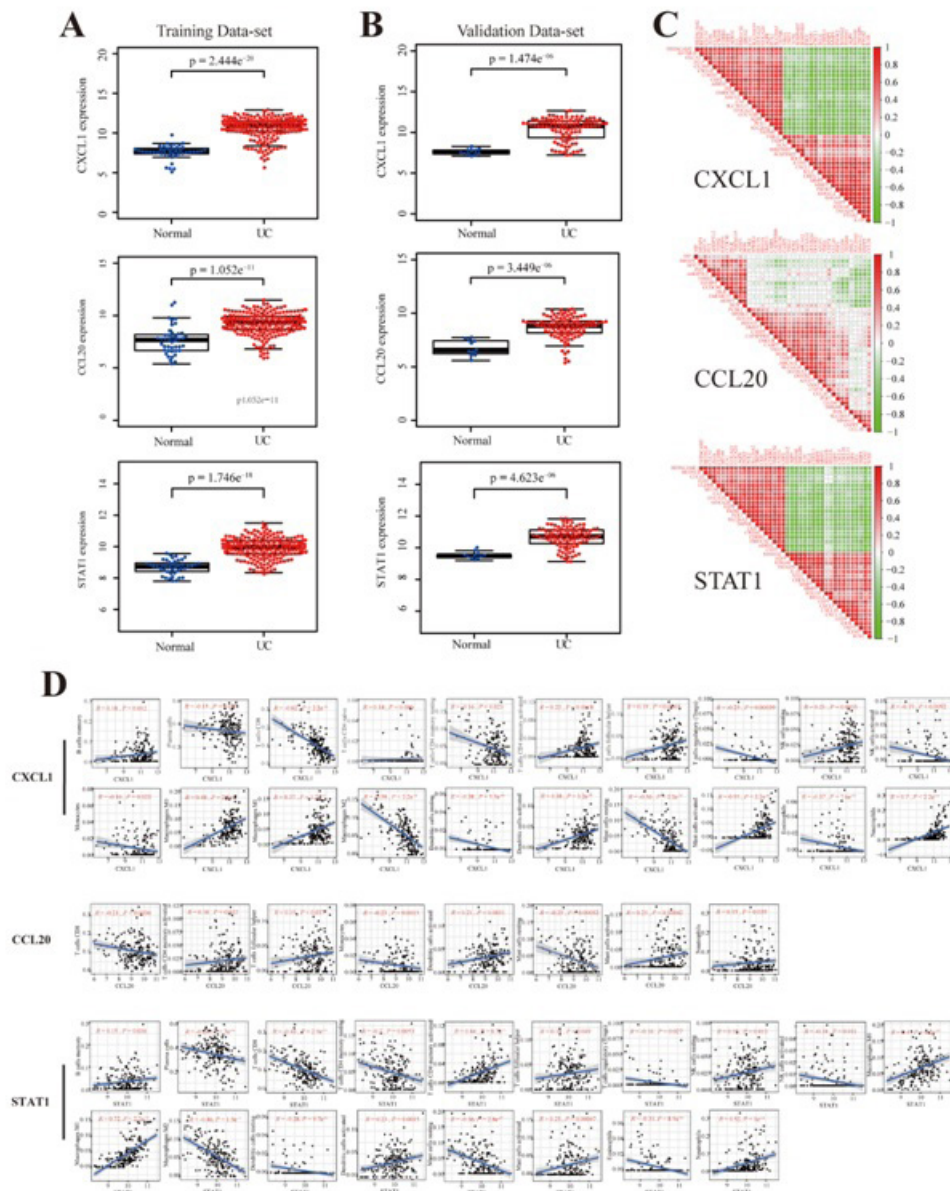


**Figure 4.** (A) The expression of HUB genes in the training dataset showed that CXCL1( $p = 2.44e-20$ ), CCL20( $p = 1.052e-11$ ), and STAT1( $p = 1.746e-18$ ) were all highly expressed in UC samples. (B) The expression of HUB genes in the validation dataset showed that CXCL1( $p = 1.474e-06$ ), CCL20( $p = 3.449e-06$ ), and STAT1( $p = 4.623e-06$ ) were all highly expressed in UC samples. (C) Correlation analysis of the top 20 DEGs in UC samples of both high and low expression groups in the training dataset. Red represents positive correlation of the DEGs, while green represents negative correlation of the DEGs. (D) positively correlated with immune cells ;  $R < 0$ , gene expression being negatively correlated with immune cells).

**Abbreviation:** UC: Ulcerative Colitis; DEGs: Differentially Expressed Genes

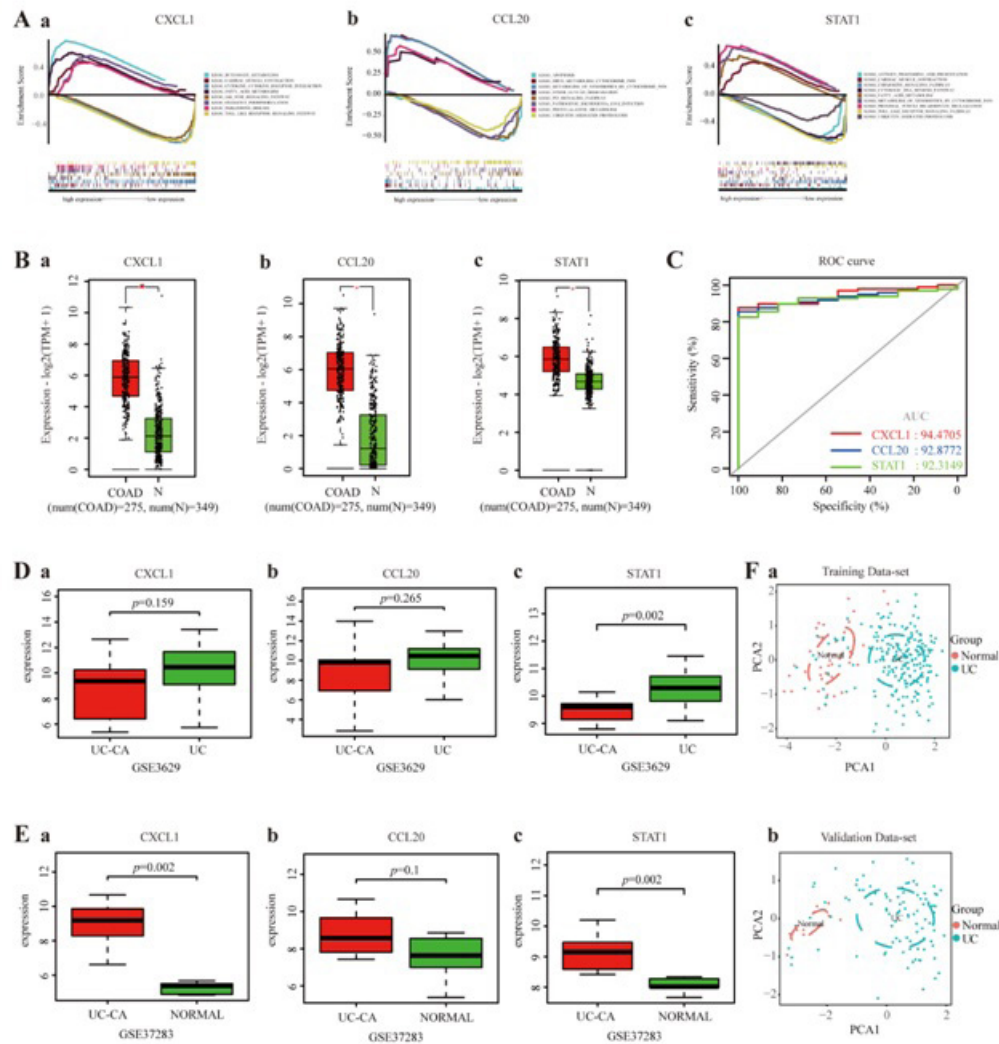


**Figure 5.** (A) GSEA analysis of the high and low expression groups in UC samples from the training dataset. (B) When compared to the normal samples, CXCL1, CCL20 and STAT1 all displayed a higher expression level in the COAD samples. (C) ROC curves drawn for the validation dataset based on the expression levels of CXCL1, CCL20 and STAT1 (CXCL1(AUG=94.4705), CCL20(AUG=92.8772), STAT1(AUG=92.3149)). (D) The expression difference of HUB genes in UC and UC-CA samples of the GSE3629 dataset, and expression of CXCL1 ( $p = 0.159$ ) and CCL20 ( $P = 0.265$ ) showed no statistical significance in UC and UC-CA samples, STAT1 ( $P = 0.002$ ) was highly expressed in UC samples. (E) The expression difference of HUB genes in UC and normal samples of the GSE37283 dataset: CXCL1 ( $P = 0.002$ ) and STAT1 ( $P = 0.002$ ) were highly expressed in UC-CA samples, no statistical significance was detected in the expression of CCL20 ( $P = 0.1$ ) in both UC-CA and normal samples. (F) PCA analysis of the training dataset and the validation dataset.

**Abbreviation:** UC: Ulcerative Colitis; UC-CA: UC-Related Cancer

### 3.6. Correlation of CXCL1, CCL20 and STAT1 Expression with Colorectal Cancer

Based on correlation analysis in the GEPIA2 database, CXCL1, CCL20 and STAT1 were all highly expressed in COAD samples compared to normal tissues (Figure 5B). We then further explore HUB genes expression in UC and UC-CA samples. The expression of CXCL1, CCL20 and STAT1 was analyzed in the GSE3629 dataset (Figure 5D), which turned out except for the high expression of STAT1 in the UC sample, and no statistical difference showed in the expression of CXCL1 and CCL20 in UC and UC-CA (Ulcerative colitis associated cancer samples. However, when

regarded to the GSE37283 dataset, as was shown in Figure 5E the expression of HUB genes in normal and UC-CA samples, CXCL1 and STAT1 were both highly expressed in UC-CA samples ( $P = 0.002$ ), while CCL20 expression displayed no significant difference between normal and UC-CA samples. ( $p = 0.1$ ) Immunohistochemistry (IHC) was performed to detect the expression of CXCL1, CCL20, and STAT1 proteins in CRC tissues and their corresponding surgical margin tissues, and we found that the expression of CXCL1, CCL20, and STAT1 proteins in CRC tissues was higher than that in their corresponding surgical margin tissues (Figure 6B).

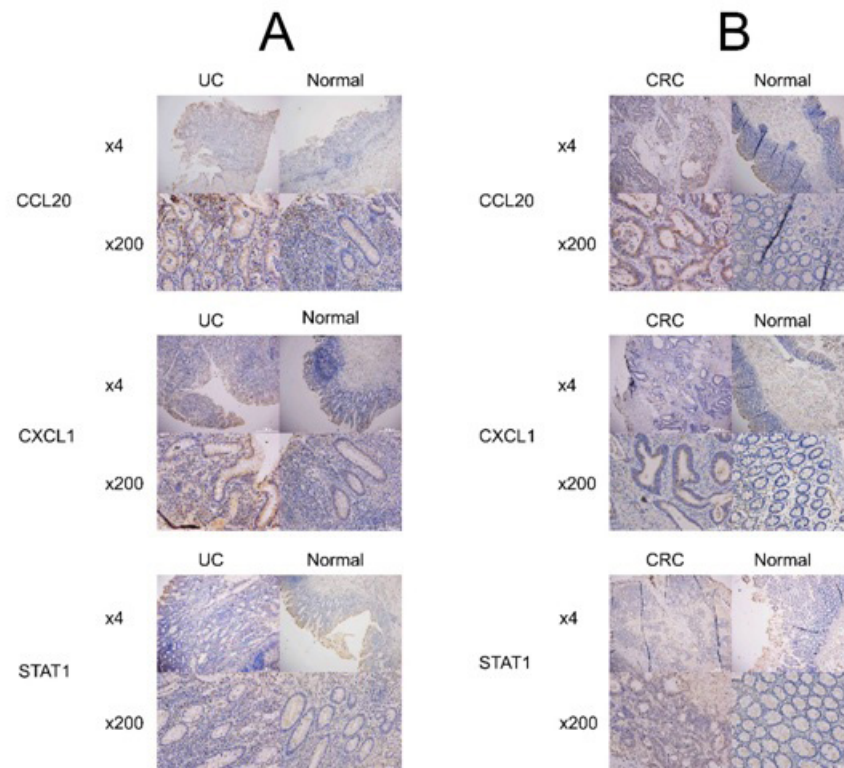


**Figure 6.**(A) Immunohistochemistry in UC tissues and their corresponding surgical margin tissues. (B) Immunohistochemistry in CRC tissues and their corresponding surgical margin tissues.

### 3.7. Analysis of Immune Infiltration

According to recent immunological reports, CIBERSORT, an estimate immune cell subsets through deconvolution algorithm performed on solid tumor samples, has been applied in relevant studies of cancer microenvironment [28, 29]. In our study, CIBERSORT was applied to assess the relative proportions of 22 different immune cells in the training dataset of every sample. Figure 7A,B summarized the abundance of immune cells in normal samples and UC samples using CIBERSORT, and the expression levels of infiltrated immune cells in two groups were presented as different. The followings processed a higher expression level in UC samples: B cells naive ( $p < 0.001$ ), Plasma cells ( $p < 0.001$ ), T cells CD4 memory activated ( $p = 0.001$ ), NK cells resting ( $p < 0.001$ ), Macrophages M0 ( $p < 0.001$ ), Macrophages M1 ( $p < 0.001$ ), Dendritic cells activated ( $p < 0.001$ ), Mast cells activated ( $p = 0.004$ ), Neutrophils ( $p < 0.001$ ), whereas B cells memory ( $p = 0.005$ ), T cells CD8 ( $p =$

$0.005$ ), T cells CD4 memory resting ( $p = 0.01$ ), T cells regulatory (Tregs) ( $p = 0.007$ ), T cells gamma delta ( $p = 0.003$ ), NK cells activated ( $p < 0.001$ ), Macrophages M2 ( $p < 0.001$ ), Dendritic cells resting ( $p < 0.001$ ), Mast cells resting ( $p < 0.001$ ), Eosinophils ( $p < 0.001$ ) were highly expressed in normal samples. And T cells helper ( $p = 0.135$ ), T cells CD4 naïve ( $p = 0.308$ ), and Monocytes ( $p = 0.965$ ) were not statistically different from each other. Correlation analysis of the immune cells was shown in (Figure 7C), where the positive correlation was shown in red while the negative correlation in green. From PCA, the proportion of immune cells between the normal and UC samples in the training dataset showed significant group bias clustering and individual differences. Correlation tests on HUB genes' immune cells were conducted so information can be obtained on how expression levels of HUB genes and immune cell content relate to each other. (Figure 7D) (Table S4).

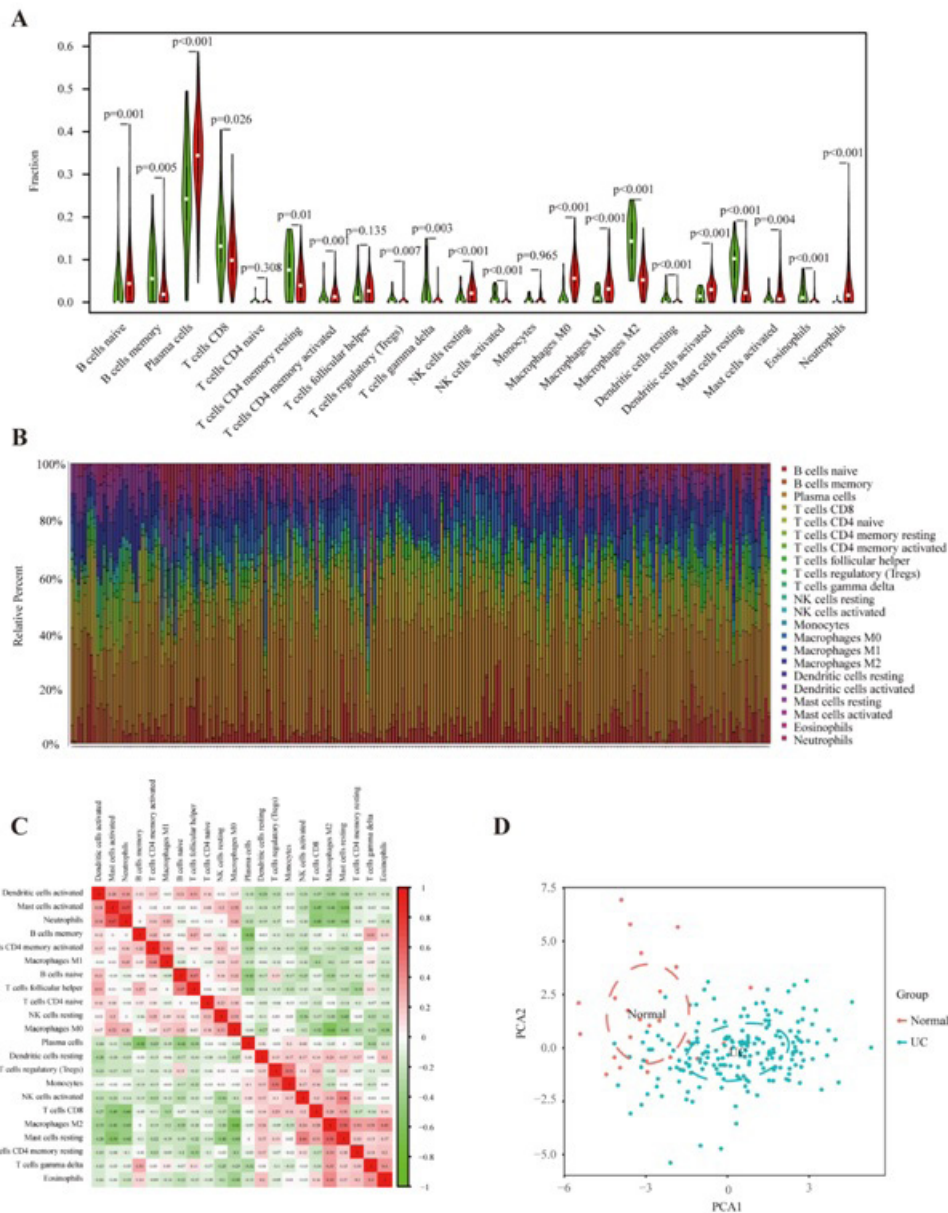


**Figure 7.**(A) Differences in immune infiltration between the UC and normal samples of the training dataset (the normal samples as green, the UC samples as red, and  $p < 0.05$  was considered statistically significant). (B) Relative abundance of the 22 immune cell subsets from the 246 samples in the training dataset. (C) Correlation analysis of the immune cells (red for positive correlation and green for negative correlation). (D) PCA analysis of the 246 samples in the training dataset.

**Table 4:** KEGG analysis.

term.id	term.name	p.adjust
hsa04062	Chemokine signaling pathway	3.27E-08
hsa04061	Viral protein interaction with cytokine and cytokine receptor	1.47E-07
hsa04657	IL-17 signaling pathway	2.68E-06
hsa04060	Cytokine-cytokine receptor interaction	7.65E-06
hsa04668	TNF signaling pathway	1.28E-04
hsa05120	Epithelial cell signaling in Helicobacter pylori infection	3.70E-04
hsa05323	Rheumatoid arthritis	9.55E-04
hsa05167	Kaposi sarcoma-associated herpesvirus infection	9.55E-04
hsa05146	Amoebiasis	9.55E-04
hsa04064	NF-kappa B signaling pathway	9.55E-04

hsa04620	Toll-like receptor signaling pathway	9.55E-04
hsa05134	Legionellosis	2.69E-03
hsa04621	NOD-like receptor signaling pathway	6.67E-03
hsa05169	Epstein-Barr virus infection	8.38E-02
hsa05140	Leishmaniasis	8.88E-02
hsa05145	Toxoplasmosis	1.68E-01
hsa04270	Vascular smooth muscle contraction	2.21E-01

Table 5-1: GSEA (CXCL1).

pathway	NES	NOM p-val
KEGG TOLL LIKE RECEPTOR SIGNALING PATHWAY	-1.73E+00	0.00E+00
KEGG JAK STAT SIGNALING PATHWAY	-1.70E+00	0.00E+00
KEGG PANCREATIC CANCER	-1.65E+00	0.00E+00
KEGG PROXIMAL TUBULE BICARBONATE RECLAMATION	1.61E+00	0.00E+00
KEGG HEMATOPOIETIC CELL LINEAGE	-1.64E+00	1.95E-03
KEGG OXIDATIVE PHOSPHORYLATION	2.07E+00	1.96E-03
KEGG CYTOKINE CYTOKINE RECEPTOR INTERACTION	-1.68E+00	1.96E-03
KEGG LEISHMANIA INFECTION	-1.65E+00	1.97E-03
KEGG CHRONIC MYELOID LEUKEMIA	-1.74E+00	1.98E-03
KEGG TYPE I DIABETES MELLITUS	-1.64E+00	2.01E-03
KEGG SMALL CELL LUNG CANCER	-1.63E+00	2.01E-03
KEGG EPITHELIAL_CELL_SIGNALING_IN_HELICOBACTER_PYLORI_INFECTION	-1.83E+00	2.02E-03
KEGG BUTANOATE METABOLISM	1.75E+00	2.04E-03
KEGG PATHWAYS IN CANCER	-1.59E+00	2.05E-03
KEGG CYTOSOLIC DNA SENSING PATHWAY	-1.69E+00	3.85E-03
KEGG CARDIAC MUSCLE CONTRACTION	1.76E+00	3.97E-03
KEGG AUTOIMMUNE THYROID DISEASE	-1.77E+00	4.03E-03
KEGG CHEMOKINE SIGNALING PATHWAY	-1.67E+00	5.74E-03
KEGG COMPLEMENT AND COAGULATION CASCADES	-1.59E+00	5.88E-03
KEGG VIRAL MYOCARDITIS	-1.78E+00	5.94E-03
KEGG GRAFT VERSUS HOST DISEASE	-1.59E+00	6.02E-03
KEGG FC GAMMA R MEDIATED PHAGOCYTOSIS	-1.66E+00	7.94E-03
KEGG CITRATE CYCLE TCA CYCLE	1.82E+00	8.06E-03
KEGG FOCAL ADHESION	-1.62E+00	1.00E-02
KEGG NATURAL KILLER CELL MEDIATED CYTOTOXICITY	-1.69E+00	1.01E-02
KEGG FATTY ACID METABOLISM	1.66E+00	1.02E-02
KEGG GLYCOLYSIS GLUCONEOGENESIS	1.66E+00	1.02E-02
KEGG RENAL CELL CARCINOMA	-1.65E+00	1.04E-02
KEGG NOD LIKE RECEPTOR SIGNALING PATHWAY	-1.64E+00	1.19E-02
KEGG INTESTINAL IMMUNE NETWORK FOR IGA PRODUCTION	-1.61E+00	1.20E-02
KEGG ACUTE MYELOID LEUKEMIA	-1.64E+00	1.40E-02
KEGG PROPANOATE METABOLISM	1.76E+00	1.41E-02
KEGG APOPTOSIS	-1.58E+00	1.47E-02
KEGG METABOLISM OF XENOBIOTICS BY CYTOCHROME P450	1.59E+00	1.58E-02
KEGG ALLOGRAFT REJECTION	-1.62E+00	1.59E-02
KEGG GLYCOSAMINOGLYCAN DEGRADATION	-1.66E+00	1.78E-02
KEGG TYROSINE METABOLISM	1.62E+00	1.78E-02
KEGG ECM RECEPTOR INTERACTION	-1.62E+00	1.79E-02
KEGG LEUKOCYTE TRANSENDOTHELIAL MIGRATION	-1.55E+00	1.83E-02
KEGG TERPENOID BACKBONE BIOSYNTHESIS	1.53E+00	1.94E-02
KEGG MATURITY ONSET DIABETES OF THE YOUNG	1.49E+00	1.95E-02
KEGG PATHOGENIC ESCHERICHIA COLI INFECTION	-1.59E+00	2.18E-02
KEGG NITROGEN METABOLISM	1.50E+00	2.34E-02
KEGG FC EPSILON RI SIGNALING PATHWAY	-1.57E+00	2.35E-02
KEGG PPAR SIGNALING PATHWAY	1.47E+00	2.35E-02
KEGG RIG I LIKE RECEPTOR SIGNALING PATHWAY	-1.60E+00	2.43E-02
KEGG CELL ADHESION MOLECULES CAMS	-1.56E+00	2.57E-02
KEGG PORPHYRIN AND CHLOROPHYLL METABOLISM	1.56E+00	2.58E-02
KEGG ANTIGEN PROCESSING AND PRESENTATION	-1.68E+00	2.79E-02
KEGG DRUG METABOLISM CYTOCHROME P450	1.53E+00	2.85E-02
KEGG PARKINSONS DISEASE	1.81E+00	3.17E-02
KEGG RETINOL METABOLISM	1.53E+00	3.23E-02

KEGG UBIQUITIN MEDIATED PROTEOLYSIS	-1.60E+00	3.25E-02
KEGG BETA ALANINE METABOLISM	1.57E+00	3.54E-02
KEGG GLIOMA	-1.49E+00	3.56E-02
KEGG PYRUVATE METABOLISM	1.64E+00	3.64E-02
KEGG VALINE LEUCINE AND ISOLEUCINE_DEGRADATION	1.61E+00	3.85E-02
KEGG MTOR SIGNALING PATHWAY	-1.41E+00	4.03E-02
KEGG ENDOCYTOSIS	-1.38E+00	4.11E-02
KEGG HYPERTROPHIC CARDIOMYOPATHY HCM	-1.45E+00	4.39E-02
KEGG B CELL RECEPTOR SIGNALING PATHWAY	-1.59E+00	4.44E-02
KEGG COLORECTAL CANCER	-1.52E+00	4.46E-02
KEGG PRIMARY BILE ACID BIOSYNTHESIS	1.42E+00	4.53E-02
KEGG GLYCOSAMINOGLYCAN BIOSYNTHESIS CHONDROITIN SULFATE	-1.52E+00	4.55E-02
KEGG GLYCOSYLPHOSPHATIDYLINOSITOL GPI ANCHOR BIOSYNTHESIS	1.60E+00	4.64E-02

Table 5-2: GSEA (CCL20)

pathway	NES	NOM p-val
KEGG APOPTOSIS	-1.69E+00	0.00E+00
KEGG UBIQUITIN MEDIATED PROTEOLYSIS	-1.84E+00	1.97E-03
KEGG P53 SIGNALING PATHWAY	-1.67E+00	3.91E-03
KEGG PATHOGENIC ESCHERICHIA COLI INFECTION	-1.60E+00	9.71E-03
KEGG GLYCOSAMINOGLYCAN BIOSYNTHESIS KERATAN SULFATE	-1.54E+00	1.55E-02
KEGG TYPE I DIABETES MELLITUS	-1.54E+00	2.52E-02
KEGG_EPITHELIAL_CELL_SIGNALING_IN_HELICOBACTER_PYLORI_INFECTION	-1.54E+00	2.61E-02
KEGG AMYOTROPHIC LATERAL SCLEROSIS ALS	-1.38E+00	2.74E-02
KEGG NOD LIKE RECEPTOR SIGNALING PATHWAY	-1.56E+00	3.01E-02
KEGG TYPE II DIABETES MELLITUS	-1.43E+00	3.01E-02
KEGG VIBRIO CHOLERAEE INFECTION	-1.55E+00	3.05E-02
KEGG GRAFT VERSUS HOST DISEASE	-1.48E+00	4.09E-02
KEGG PYRIMIDINE METABOLISM	-1.58E+00	4.24E-02
KEGG_GLYCOPHINGOLIPID_BIOSYNTHESIS_LACTO_AND_NEOLACTO_SERIES	-1.46E+00	4.37E-02
KEGG OOCYTE MEIOSIS	-1.49E+00	4.54E-02
KEGG GLYCOPHINGOLIPID BIOSYNTHESIS GANGLIO SERIES	-1.50E+00	4.82E-02
KEGG PROTEASOME	-1.66E+00	4.87E-02
KEGG TAURINE AND HYPOTAURINE METABOLISM	1.63E+00	1.31E-02
KEGG METABOLISM OF XENOBIOTICS BY CYTOCHROME P450	1.48E+00	2.52E-02
KEGG OTHER GLYCAN DEGRADATION	1.57E+00	2.70E-02
KEGG DRUG METABOLISM CYTOCHROME P450	1.45E+00	3.44E-02
KEGG PHENYLALANINE METABOLISM	1.45E+00	4.60E-02

Table 5-3: GSEA (STAT1)

pathway	NES	NOM p-val
KEGG RETINOL METABOLISM	1.59E+00	6.15E-03
KEGG PROXIMAL TUBULE BICARBONATE RECLAMATION	1.60E+00	8.28E-03
KEGG CARDIAC MUSCLE CONTRACTION	1.73E+00	9.84E-03
KEGG FATTY ACID METABOLISM	1.59E+00	2.03E-02
KEGG METABOLISM OF XENOBIOTICS BY CYTOCHROME P450	1.54E+00	2.07E-02
KEGG OXIDATIVE PHOSPHORYLATION	1.83E+00	2.20E-02
KEGG NITROGEN METABOLISM	1.53E+00	2.50E-02
KEGG DRUG METABOLISM CYTOCHROME P450	1.51E+00	2.51E-02
KEGG PPAR SIGNALING PATHWAY	1.40E+00	3.74E-02
KEGG MATURITY ONSET DIABETES OF THE YOUNG	1.49E+00	4.60E-02
KEGG ANTIGEN PROCESSING AND PRESENTATION	-1.90E+00	0.00E+00
KEGG_EPITHELIAL_CELL_SIGNALING_IN_HELICOBACTER_PYLORI_INFECTION	-1.81E+00	0.00E+00
KEGG VIRAL MYOCARDITIS	-1.79E+00	0.00E+00
KEGG PROTEASOME	-1.79E+00	0.00E+00
KEGG AUTOIMMUNE THYROID DISEASE	-1.73E+00	0.00E+00
KEGG LEISHMANIA INFECTION	-1.71E+00	0.00E+00
KEGG TOLL LIKE RECEPTOR SIGNALING PATHWAY	-1.81E+00	2.01E-03
KEGG CYTOKINE CYTOKINE RECEPTOR INTERACTION	-1.67E+00	2.04E-03



KEGG INTESTINAL IMMUNE NETWORK FOR IGA PRODUCTION	-1.67E+00	2.04E-03
KEGG CYTOSOLIC DNA SENSING PATHWAY	-1.77E+00	2.05E-03
KEGG CHEMOKINE SIGNALING PATHWAY	-1.76E+00	2.05E-03
KEGG TRYPTOPHAN METABOLISM	-1.58E+00	3.85E-03
KEGG FC GAMMA R MEDIATED PHAGOCYTOSIS	-1.78E+00	3.94E-03
KEGG CELL ADHESION MOLECULES CAMS	-1.63E+00	4.03E-03
KEGG HEMATOPOIETIC CELL LINEAGE	-1.58E+00	4.07E-03
KEGG JAK STAT SIGNALING PATHWAY	-1.67E+00	4.10E-03
KEGG NATURAL KILLER CELL MEDIATED CYTOTOXICITY	-1.71E+00	4.11E-03
KEGG NOD LIKE RECEPTOR SIGNALING PATHWAY	-1.77E+00	4.12E-03
KEGG UBIQUITIN MEDIATED PROTEOLYSIS	-1.75E+00	5.94E-03
KEGG PANCREATIC CANCER	-1.60E+00	6.07E-03
KEGG ASTHMA	-1.65E+00	7.86E-03
KEGG SMALL CELL LUNG CANCER	-1.56E+00	8.13E-03
KEGG PRION DISEASES	-1.60E+00	8.16E-03
KEGG GRAFT VERSUS HOST DISEASE	-1.58E+00	8.18E-03
KEGG COMPLEMENT AND COAGULATION CASCADES	-1.58E+00	8.21E-03
KEGG APOPTOSIS	-1.63E+00	9.80E-03
KEGG B CELL RECEPTOR SIGNALING PATHWAY	-1.70E+00	1.02E-02
KEGG T CELL RECEPTOR SIGNALING PATHWAY	-1.74E+00	1.02E-02
KEGG TYPE I DIABETES MELLITUS	-1.63E+00	1.05E-02
KEGG P53 SIGNALING PATHWAY	-1.56E+00	1.40E-02
KEGG LEUKOCYTE TRANSENDOTHELIAL MIGRATION	-1.57E+00	1.42E-02
KEGG PATHWAYS IN CANCER	-1.48E+00	1.46E-02
KEGG FC EPSILON RI SIGNALING PATHWAY	-1.61E+00	1.60E-02
KEGG PRIMARY IMMUNODEFICIENCY	-1.61E+00	1.63E-02
KEGG ALLOGRAFT REJECTION	-1.61E+00	1.67E-02
KEGG CELL CYCLE	-1.73E+00	1.80E-02
KEGG RIG I LIKE RECEPTOR SIGNALING PATHWAY	-1.69E+00	1.83E-02
KEGG CHRONIC MYELOID LEUKEMIA	-1.57E+00	1.87E-02
KEGG PATHOGENIC ESCHERICHIA COLI INFECTION	-1.61E+00	1.97E-02
KEGG FOCAL ADHESION	-1.53E+00	2.45E-02
KEGG ECM RECEPTOR INTERACTION	-1.50E+00	4.81E-02

**Table 6:** Immune cell correlation.

Immune cell	p-value		
	CXCL1	CCL20	STAT1
B cells memory	1.23E-02	-	3.63E-02
Plasma cells	3.70E-02	-	7.00E-04
T cells CD8	3.47E-22	3.61E-03	2.88E-10
T cells CD4 naive	4.65E-02	-	-
T cells CD4 memory resting	2.29E-02	-	5.34E-03
T cells CD4 memory activated	1.85E-03	1.16E-02	8.71E-11
T cells follicular helper	6.51E-03	1.16E-02	4.91E-02
T cells regulatory (Tregs)	3.95E-04	-	2.67E-02
NK cells resting	3.47E-03	-	1.33E-02
NK cells activated	9.22E-03	-	1.06E-02
Monocytes	2.30E-02	1.51E-03	-
Macrophages M0	2.58E-12	-	6.18E-09
Macrophages M1	1.18E-07	-	6.90E-32
Macrophages M2	6.94E-19	-	1.93E-11
Dendritic cells resting	5.50E-08	-	9.73E-05
Dendritic cells activated	3.25E-08	3.11E-03	1.53E-03
Mast cells resting	2.45E-17	5.16E-04	2.81E-07
Mast cells activated	1.21E-16	4.24E-04	4.69E-04
Eosinophils	7.59E-08	-	8.88E-06
Neutrophils	2.37E-30	3.86E-02	1.02E-14

#### 4. Discussion

It has long been recognized that the pathogenesis of UC is closely linked to immune response. However, no relevant analysis and research on UC's immune-related genes from the perspective of bioinformatics [7]. Although recent findings of biomarkers has made great contribution to improve UC-related diagnosis and treatment [30-32], such as immunologic factors and the complexity of biology into account, the poor prognosis of UC calls for an urgent need to further understand the mechanism of UC and find strong biomarkers for providing a new method for the diagnosis and treatment of UC.

25 overlapping genes were chosen as IRDEGs from three database. GO and KEGG analysis demonstrated IRDEGs' main participation in antimicrobial humoral response, zymogen granule, chemokine signaling pathway, etc. Associated studies indicate that biological functions and pathways concerning IRDEGs are related to the diagnosis and treatment of UC [33-36]. HUB genes (CXCL1, CCL20, STAT1) were identified by STRING and Cytoscape for next-step verification. CXCL1 is an antimicrobial gene that encodes a protein that belongs to the CXC subfamily of chemokines, and this very protein being a secretory growth factor. Abnormal expression of this protein is connected the growth and development of certain tumors [37]. CCL20 is an antimicrobial gene and a member of the Small Inducible Cytokine Subfamily A (Cys-Cys). Cytokines are a family of secretory proteins involved in immune regulation and inflammatory processes [38]. STAT1 encodes a protein that is a member of the STAT protein family and functions to mediate cellular responses to cytokines and growth factors. This protein mediates the expression of a set of genes and is thought to be crucial for cell survival under different cell stimuli and pathogen stimuli [39]. CXCL1, CCL20 and STAT1 were highly expressed in the UC samples of the training dataset and the validation dataset. What's more, ROC curve showed that HUB genes showed good power to diagnose UC. And in in corresponding to ROC, PCA showed HUB gene can distinguish UC samples from normal samples. Therefore, all the before-mentioned evidence makes it possible for HUB gene to become a key biomarker for UC diagnosis. According to the results of GEPIA2 database, HUB genes were highly expressed in CRC samples in contrast with the normal samples. This was consistent with the expression results of CXCL1 and STAT1 in GSE37283 dataset. Nevertheless, no significant intergroup statistical difference was shown for the CCL20 expression in datasets, which may due to the small sample size, thus requesting verification by expanding the sample size in the follow-up research.

Previous studies has showed that CXCL1 play a role by binding specifically to C-X-C Motif Chemokine Receptor 2 (CXCR2) [40]. The CXCL1 / CXCR2 signaling pathway not only regulates inflammatory responses, but also induces tumor proliferation, angiogenesis and lymphoangiogenesis; additionally, it accelerates

tumor invasion and vascular metastasis. In sum, CXCL1 / CXCR2, through chemokine signaling pathway and inflammatory response, may play a key role in the development of UC [32, 41]. Overexpression of CCL20 and its receptor CCR6 was observed in active inflammatory bowel disease whilst both could be found in epithelium and infiltrating immune cells in lamina propria. Apart from that, a study showed CCL20 may prolong the inflammatory response to ulcerative colitis [42, 43]. Moreover, there were interactions between CCL20 and CCR6 observed to play a physiologically important role in colonic mucosa. It has been reported the chemokine receptor CCR6 is expressed in colorectal cancer and several other cancer types, and stimulation by its physiological chemokine ligand CCL20 has been reported to promote cancer cell proliferation and migration in vitro [44]. Furthermore, a previous study has suggested that CCL20 and its receptor, CCR6, were significantly correlated with the development of multiple colorectal malignancies [45]. Lei et al. indicated an activated colonic renin-angiotensin system (RAS) in colitis, which can promote the activation of TH17 via JAK2/STAT pathway [46]. An earlier study showed that ulcerative colitis remarkably heightens the expression and activation of STAT1. Therefore, STAT1 may be crucial to the pathophysiology of colonic inflammation [47]. Kaler et al. confirmed that silencing of STAT1 in tumor cells cuts off its crosstalk with fibroblasts, suggesting STAT1 is a novel link between intestinal inflammation and colon cancer [48].

After the monogenic GSEA analysis performed on HUB genes, we concluded that the significantly changed pathways between the high-low expression groups are mainly concentrated in chemokine signaling pathway, JAK/STAT signaling pathway, cell apoptosis, toll-like receptor signaling pathway, etc. MicroRNA 15A and 16-1 activate signaling pathways that mediate immune regulation of B-cell's chemotaxis to colorectal tumors [49]. Obesity exacerbates colitis-associated cancer via IL-6-regulated macrophage polarisation and CCL-20/CCR-6-mediated lymphocyte recruitment [50]. Genetic variation in the JAK/STAT/SOCS-signaling pathway appears to be associated with both colon and rectal cancer risk. This impact on cancer goes beyond effects components of the pathway cast respectively on risk, and encompasses additional risk associated with interaction of genetic and lifestyle factors [51]. p53-up-regulated modulator of apoptosis (PUMA)-mediated intestinal epithelial apoptosis contributes to ulcerative colitis in humans and mice [52]. Raf kinase inhibitor proteins mediate human and mouse intestinal epithelial cells' apoptosis and promote IBDs [53]. Toll-like receptors (TLRs), who is actually an innate immune sensors family, play an important part in defending against pathogens and take part in of IBD pathogenesis [54]. The pathways mentioned above have been proved to be closely related to the pathogenesis of UC and UC-CRC in previous studies. And these studies has obtained the overlapping results of CXCL1, CCL20 and STAT1 in the bioinformatic level of our study, indicating that CXCL1,

CCL20 and STAT1 may have great statistical efficiency and biological function concerning UC tissues, providing some new thinking for the immunotherapy of UC.

According to the analysis of immune infiltration, Naive B cells, Plasma cells, T cells CD4 memory activated, NK cells, Macrophages M0, Macrophages M1, Dendritic cells activated, Mast cells activated, and Neutrophils expressed highly in UC samples in comparison with normal samples. The potential link between immune cells and UC has been suggested in prior studies: Percentages of naive B cells were reported to be increased in Crohn's disease and ulcerative colitis [55]. Mucosal CXCR4+ IgG plasma cells promoted the pathogenic process of UC by FcγR-mediated activation of CD14 macrophages [56]. IBD patients infiltrated with T cell in their intestine were shown consisting of increased percentages of CD4+ T cells, Tregs, and TCM (Central Memory T cell) [57]. The colonic lamina propria of inflammatory bowel disease patients was shown to have increased proportion of CD16(+) NK cells [58]. Macrophages are thought to have important functions in gut homeostasis with their effective ability to eliminate bacteria, foreign matter, and apoptotic cells. Under inflammatory conditions, they can release cytokines in response to TLR stimulation, thereby promoting the inflammatory response [59]. Intestinal DCs strongly express microbial receptors, and this causes rapid inflammatory responses, and the components involved in their activation/maturation and differentiation can be used as potential candidates for valuable therapeutic targets in IBD [60]. Mast cells participate in the activation of ulcerative colitis [61, 62]. Inappropriate mucosal immune responses to normal intestinal components presents as a distinguishing feature of the pathogenesis regarding inflammatory bowel disease, which always leads to local pro-inflammatory and anti-inflammatory cytokine imbalances followed by influx of neutrophils and monocytes and secretion of oxygen free radicals and enzymes, at last resulting in tissue damage [63]. These results improve the pathogenesis of UC from the perspective of bioinformatics and are consistent with the conclusions of previous studies, indicating that HUB gene can be used as a reliable biomarker for the diagnosis of UC patients. Nevertheless, there are certain limitations in the study should be acknowledged. First, a retrospective analysis was what's been adopted in this study, where fresh frozen samples were included in samples from the training and the validation datasets. Consequently, the samples stability and validity remain to be verified, which will demand prospective cohort studies to be performed on our results. Second, the gene expression features involved in our study must have been affected by biological heterogeneity and statistical bias. Although we used the GEO dataset with a large sample size, more datasets with varied sample attributes are still needed for broader validation. Finally, the gene expression profile of prognostic markers constructed in this study was brought out based on microarray platform, which is proved difficult for wider ever day clinical practice considering its expen-

siveness, long transformation cycle and excessive requirements to bioinformatic expertise [64].

## 5. Conclusion

To conclude, a total of 25 IRDGEs and 3 HUB genes (CXCL1, CCL20, STAT1) were identified in our study. And further biological function analysis has brought us a better understanding of HUB genes' part played in the pathogenesis and progression of UC, which refers not only to their diagnostic value as biomarkers, but also to a more detailed molecular mechanism underlying the development and carcinogenesis of UC. There's a chance in the future CXCL1, CCL20 and STAT1 set up new ideas for the diagnosis and immune-related treatment of ulcerative colitis.

## 6. Abbreviation:

UC: Ulcerative Colitis; TOM: Topological Overlap Measure; DEGs: Differentially Expressed Genes.

## 7. Funding:

This work was supported by grants provided from the Natural Science Foundation of Hunan Province of China (2020JJ3054).

## References:

1. Molodecky NA, Soon IS, Rabi DM, Ghali WA, Ferris M, Chernoff G, et al. Increasing incidence and prevalence of the inflammatory bowel diseases with time, based on systematic review. *Gastroenterology*. 2012; 142: 46-54.
2. Ng SC, Shi HY, Hamidi N, Underwood FE, Tang W, Benchimol EI, et al. Worldwide incidence and prevalence of inflammatory bowel disease in the 21st century: a systematic review of population-based studies. *Lancet*. 2018; 390: 2769-78.
3. Feuerstein JD, Moss AC, Farraye FA. Ulcerative Colitis. *Mayo Clin Proc*. 2019; 94: 1357-73.
4. Biroulet PL, Sandborn W, Sands BE, Reinisch W, Bemelman W, Bryant RV, et al. Selecting Therapeutic Targets in Inflammatory Bowel Disease (STRIDE): Determining Therapeutic Goals for Treat-to-Target. *Am J Gastroenterol*. 2015; 110: 1324-38.
5. Cosnes J, Rousseau GC, Seksik P, Cortot A. Epidemiology and natural history of inflammatory bowel diseases. *Gastroenterology*. 2011; 140: 1785-94.
6. Ahluwalia B, Magnusson MK, Öhman L. Mucosal immune system of the gastrointestinal tract: maintaining balance between the good and the bad. *Scand J Gastroenterol*. 2017; 52: 1185-93.
7. Ungaro R, Mehandru S, Allen PB, Biroulet PL, Colombel JF. Ulcerative colitis. *Lancet*. 2017; 389, 1756-1770.
8. Chambers WM, Warren BF, Jewell DP, Mortensen NJ. Cancer surveillance in ulcerative colitis. *Br J Surg*. 2005; 92: 928-936.
9. Isbell G, Levin B. Ulcerative colitis and colon cancer. *Gastroenterol Clin North Am*. 1988; 17: 773-91.
10. Grivennikov SI. Inflammation and colorectal cancer: colitis-associated neoplasia. *Semin Immunopathol*. 2013; 35: 229-44.

11. Hanahan D, Weinberg RA. Hallmarks of cancer: the next generation. *Cell*. 2011; 144: 646-74.
12. Mellman I, Coukos G, Dranoff G. Cancer immunotherapy comes of age. *Nature*. 2011; 480: 480-9.
13. Kulasingam V, Diamandis EP. Strategies for discovering novel cancer biomarkers through utilization of emerging technologies. *Nat Clin Pract Oncol*. 2008; 5: 588-99.
14. Langfelder P, Horvath S. WGCNA: an R package for weighted correlation network analysis. *BMC Bioinformatics*. 2008; 9: 559.
15. Leek JT, Johnson WE, Parker HS, Jaffe AE, Storey JD. The sva package for removing batch effects and other unwanted variation in high-throughput experiments. *Bioinformatics*. 2012; 28, 882-3.
16. Ritchie ME, Phipson B, Wu D, Hu Y, Law CW, Shi W, et al. limma powers differential expression analyses for RNA-sequencing and microarray studies. *Nucleic Acids Res*. 2015; 43: 47.
17. Yip AM, Horvath S. Gene network interconnectedness and the generalized topological overlap measure. *BMC Bioinformatics*. 2007; 8: 22.
18. Langfelder P, Zhang B, Horvath S. Defining clusters from a hierarchical cluster tree: the Dynamic Tree Cut package for R. *Bioinformatics*. 2008; 24, 719-720.
19. Horvath S, Dong J. Geometric interpretation of gene coexpression network analysis. *PLoS Comput Biol*. 2008; 4: 1000117.
20. Chen H, Boutros PC. VennDiagram: a package for the generation of highly-customizable Venn and Euler diagrams in R. *BMC Bioinformatics*. 2011; 12: 35.
21. Szklarczyk D, Gable AL, Lyon D, Junge A, Wyder S, Cepas HJ, et al. STRING v11: protein-protein association networks with increased coverage, supporting functional discovery in genome-wide experimental datasets. *Nucleic Acids Res*. 2019; 47: 607-13.
22. Shannon P, Markiel A, Ozier O, Baliga NS, Wang JT, Ramage D, et al. Cytoscape: a software environment for integrated models of biomolecular interaction networks. *Genome Res*. 2003; 13: 2498-504.
23. Chin CH, Chen SH, Wu HH, Ho CW, Ko MT, Lin CY, et al. cytoHubba: identifying hub objects and sub-networks from complex interactome. *BMC Syst Biol* 8 Suppl. 2014; 4: 11.
24. Zacho A, Nielsen J, Cederqvist C. Relationship between type of tobacco used and localization of tumour in patients with gastric cancer. *Acta Chir Scand*. 1975; 141: 676-9.
25. Price AL, Patterson NJ, Plenge RM, Weinblatt ME, Shadick NA, Reich D, et al. Principal components analysis corrects for stratification in genome-wide association studies. *Nat Genet*. 2006; 38: 904-9.
26. Tang Z, Kang B, Li C, Chen T, Zhang Z. GEPIA2: an enhanced web server for large-scale expression profiling and interactive analysis. *Nucleic Acids Res* 47. 2019; 556-60.
27. Newman AM, Liu CL, Green MR, Gentles AJ, Feng W, Xu Y, et al. Robust enumeration of cell subsets from tissue expression profiles. *Nat Methods*. 2015; 12: 453-7.
28. Desmedt C, Salgado R, Fornili M, Pruneri G, Van Den Eynden G, Zoppoli G, et al. Immune Infiltration in Invasive Lobular Breast Cancer. *J Natl Cancer Inst*. 2018; 110: 768-76.
29. Ali HR, Chlon L, Pharoah PD, Markowitz F, Caldas C. Patterns of Immune Infiltration in Breast Cancer and Their Clinical Implications: A Gene-Expression-Based Retrospective Study. *PLoS Med*. 2016; 13: 1002194.
30. Shi W, Zou R, Yang M, Mai L, Ren J, Wen J, et al. Analysis of Genes Involved in Ulcerative Colitis Activity and Tumorigenesis Through Systematic Mining of Gene Co-expression Networks. *Front Physiol*. 2019; 10: 662.
31. Wang H, Zhang M, Zhang M, Wang F, Liu J, Zhao Q, et al. Carboxypeptidase A6 was identified and validated as a novel potential biomarker for predicting the occurrence of active ulcerative colitis. *J Cell Mol Med*. 2020; 24: 8803-13.
32. Zhang J, Wang X, Xu L, Zhang Z, Wang F, Tang X, et al. Investigation of Potential Genetic Biomarkers and Molecular Mechanism of Ulcerative Colitis Utilizing Bioinformatics Analysis. *Biomed Res Int*. 2020; 2020: 4921387.
33. Roggenbuck D, Reinhold D, Baumgart DC, Schierack P, Conrad K, Laass MW, et al. Autoimmunity in Crohn's Disease-A Putative Stratification Factor of the Clinical Phenotype. *Adv Clin Chem*. 2016; 77: 77-101.
34. Wendt E, Keshav S. CCR9 antagonism: potential in the treatment of Inflammatory Bowel Disease. *Clin Exp Gastroenterol*. 2015; 8, 119-130.
35. Collins FM. Cellular antimicrobial immunity. *CRC Crit Rev Microbiol*. 1978; 7: 27-91.
36. Macdermott RP, Sanderson IR, Reinecker HC. The central role of chemokines (chemotactic cytokines) in the immunopathogenesis of ulcerative colitis and Crohn's disease. *Inflamm Bowel Dis*. 1998; 4: 54-67.
37. Seifert L, Werba G, Tiwari S, Giao Ly NN, Alothman S, Alqunait D, et al. The necrosome promotes pancreatic oncogenesis via CXCL1 and Mincle-induced immune suppression. *Nature*. 2016; 532, 245-9.
38. Hillier LW, Graves TA, Fulton RS, Fulton LA, Pepin KH, Minx P, et al. Generation and annotation of the DNA sequences of human chromosomes 2 and 4. *Nature*. 2005; 434, 724-731.
39. Chen K, Liu J, Liu S, Xia M, Zhang X, Han D, et al. Methyltransferase SETD2-Mediated Methylation of STAT1 Is Critical for Interferon Antiviral Activity. *Cell*. 2017; 170: 492-506.
40. Mantovani A, Savino B, Locati M, Zammataro L, Allavena P, Bonecchi R. The chemokine system in cancer biology and therapy. *Cytokine Growth Factor Rev*. 2010; 21: 27-39.
41. Acharyya S, Oskarsson T, Vanharanta S, Malladi S, Kim J, Morris PG, et al. A CXCL1 paracrine network links cancer chemoresistance and metastasis. *Cell*. 2012; 150: 165-78.
42. Skovdahl HK, Damås JK, Granlund AVB, Østvik AE, Doseth B, Bruland T, et al. C-C Motif Ligand 20 (CCL20) and C-C Motif Chemokine Receptor 6 (CCR6) in Human Peripheral Blood Mono-

- nuclear Cells: Dysregulated in Ulcerative Colitis and a Potential Role for CCL20 in IL-1 $\beta$  Release. *Int J Mol Sci.* 2018; 19: 3257.
43. Skovdahl HK, Granlund A, Østvik AE, Bruland T, Bakke I, Torp SH, et al. Expression of CCL20 and Its Corresponding Receptor CCR6 Is Enhanced in Active Inflammatory Bowel Disease, and TLR3 Mediates CCL20 Expression in Colonic Epithelial Cells. *PLoS One.* 2015; 10: e0141710.
  44. Ghadjar P, Rubie C, Aebersold DM, Keilholz U. The chemokine CCL20 and its receptor CCR6 in human malignancy with focus on colorectal cancer. *Int J Cancer.* 2009; 125: 741-5.
  45. Hashimoto K, Saigusa S, Araki T, Tanaka K, Okita Y, Fujikawa H, et al. Correlation of CCL20 expression in rectal mucosa with the development of ulcerative colitis-associated neoplasia. *Oncol Lett.* 2013; 1271-6.
  46. He L, Du J, Chen Y, Liu C, Zhou M, Adhikari S, et al. Renin-angiotensin system promotes colonic inflammation by inducing T(H)17 activation via JAK2/STAT pathway. *Am J Physiol Gastrointest Liver Physiol.* 2019; 316: G774-84.
  47. Schreiber S, Rosenstiel P, Hampe J, Nikolaus S, Groessner B, Schotelius A, et al. Activation of signal transducer and activator of transcription (STAT) 1 in human chronic inflammatory bowel disease. *Gut.* 2002; 379-85.
  48. Kaler P, Owusu BY, Augenlicht L, Klampfer L. The Role of STAT1 for Crosstalk between Fibroblasts and Colon Cancer Cells. *Front Oncol.* 2014; 4: 88.
  49. Liu R, Lu Z, Gu J, Liu J, Huang E, Liu X, et al. MicroRNAs 15A and 16-1 Activate Signaling Pathways That Mediate Chemotaxis of Immune Regulatory B cells to Colorectal Tumors. *Gastroenterology.* 2018; 154: 637-651.e7.
  50. Wunderlich CM, Ackermann PJ, Ostermann AL, Adams-Quack P, Vogt MC, Tran ML, et al. Obesity exacerbates colitis-associated cancer via IL-6-regulated macrophage polarisation and CCL-20/CCR-6-mediated lymphocyte recruitment. *Nat Commun.* 2018; 9: 1646.
  51. Slattery ML, Lundgreen A, Kadlubar SA, Bondurant KL, Wolff RK. JAK/STAT/SOCS-signaling pathway and colon and rectal cancer. *Mol Carcinog.* 2013; 52: 155-66.
  52. Qiu W, Wu B, Wang X, Buchanan ME, Regueiro MD, Hartman DJ, et al. PUMA-mediated intestinal epithelial apoptosis contributes to ulcerative colitis in humans and mice. *J Clin Invest.* 2011; 121: 1722-32.
  53. Lin W, Ma C, Su F, Jiang Y, Lai R, Zhang T, et al. Raf kinase inhibitor protein mediates intestinal epithelial cell apoptosis and promotes IBDs in humans and mice. *Gut.* 2017; 66: 597-610.
  54. Fernandes P, Macsharry J, Darby T, Fanning A, Shanahan F, Houston A, et al. Differential expression of key regulators of Toll-like receptors in ulcerative colitis and Crohn's disease: a role for Tollip and peroxisome proliferator-activated receptor gamma? *Clin Exp Immunol.* 2016; 183: 358-68.
  55. Rabe H, Malmquist M, Barkman C, Östman S, Gjertsson I, Saalman R, et al. Distinct patterns of naive, activated and memory T and B cells in blood of patients with ulcerative colitis or Crohn's disease. *Clin Exp Immunol.* 2019; 197: 111-29.
  56. Uo M, Hisamatsu T, Miyoshi J, Kaito D, Yoneno K, Kitazume MT, et al. Mucosal CXCR4+ IgG plasma cells contribute to the pathogenesis of human ulcerative colitis through Fc $\gamma$ R-mediated CD14 macrophage activation. *Gut.* 2013; 62: 1734-44.
  57. Smids C, Horjus Talabur Horje CS, Drylewicz J, Roosenboom B, Groenen MJM, Van Koolwijk E, et al. Intestinal T Cell Profiling in Inflammatory Bowel Disease: Linking T Cell Subsets to Disease Activity and Disease Course. *J Crohns Colitis.* 2018; 12: 465-75.
  58. Steel AW, Mela CM, Lindsay JO, Gazzard BG, Goodier MR. Increased proportion of CD16(+) NK cells in the colonic lamina propria of inflammatory bowel disease patients, but not after azathioprine treatment. *Aliment Pharmacol Ther.* 2011; 33: 115-26.
  59. Gren ST, Grip O. Role of Monocytes and Intestinal Macrophages in Crohn's Disease and Ulcerative Colitis. *Inflamm Bowel Dis.* 2016; 22: 1992-8.
  60. Kim WS, Song HY, Mushtaq S, Kim JM, Byun EH, Yuk JM, et al. Therapeutic Potential of Gamma-Irradiated Resveratrol in Ulcerative Colitis via the Anti-Inflammatory Activity and Differentiation of Tolerogenic Dendritic Cells. *Cell Physiol Biochem.* 2019; 52: 1117-38.
  61. Stasikowska-Kanicka O, Danilewicz M, Głowacka A, Wągrowka-Danilewicz M. Mast cells and eosinophils are involved in activation of ulcerative colitis. *Adv Med Sci.* 2012; 57: 230-6.
  62. Boeckxstaens G. Mast cells and inflammatory bowel disease. *Curr Opin Pharmacol.* 2015; 25: 45-9.
  63. Brown SJ, Mayer L. The immune response in inflammatory bowel disease. *Am J Gastroenterol.* 2007; 102: 2058-69.
  64. Wu J, Zhao Y, Zhang J, Wu Q, Wang W. Development and validation of an immune-related gene pairs signature in colorectal cancer. *Oncoimmunology.* 2019; 8: 1596715.